2019 SUMMER SCHOOL ON NEUROREHABILITATION

SUMMER SCHOOL ON NEUROREHABILITATION (SSNR2019)

Proceedings

September 15-20,

2019 Baiona (Spain)

NRG INSTITUTO CAJAL CSIC Imperial College London

Optimal Linear Filtering for Modelling the Dynamic Integration of Touch and Proprioception for Hand Movement Control

Gemma Carolina Bettelani[1], Simone Ciotti[2], Antonio Bicchi[1,3], Alessandro Moscatelli[2] and Matteo Bianchi[1]

I. Introduction

Touch provides an important cue to perceive the physical properties of the objects. Recent studies showed that tactile sensation also contributes to our sense of hand position and displacement in perceptual tasks. In our previous works [1],[2], we have shown that touch provides auxiliary cues to guide hand displacement. In fact, when we slide our finger over a ridged surface, cutaneous touch affects the direction of the active movement of the hand. In particular, according with the tactile flow model ([3],[4]), tactile feedback produces an illusory sensation of bending toward the direction perpendicular to the ridges (contribution of the touch, explained by the tactile flow model), which is integrated with the direction estimation provided from classical muscular-skeletal proprioception (unbiased). This triggers a correction of the movement in the opposite direction (Fig. 1). In Fig. 2 we report the average trajectories of the hand motion, obtained from an exemplary participant sliding their finger on a plate with different ridges orientations. When the ridges orientation is negative (clockwise rotation), the participant deviated toward right with respect to the mid-line of the plate and vice-versa. This result is in accordance with the illusory effect expressed above.

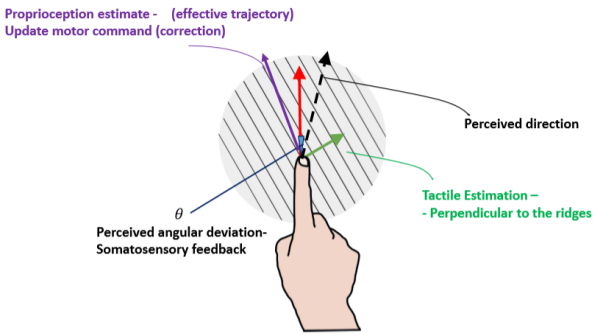

Figure 1: When a participant moved the index finger on a plate with oblique ridges, along the direction indicated by the solid red arrow (straight path), according to the model of tactile flow, the cutaneous feedback produced an illusory sensation of bending towards a direction perpendicular to the ridges (dashed black line). This eventually led to an adjustment of the motion trajectory towards a direction opposite to the one arisen from the estimate provided by the tactile flow (solid violet arrow).

II. Kalman filter model

Ideal observer models based on Kalman filtering have been often used to explain human behavior in different motor tasks

[1]Research Center "Enrico Piaggio", University of Pisa, Largo Lucio Lazzarino 1, 56126 Pisa, Italy and Department of Information Engineering, University of Pisa, via G. Caruso, 16, 56122 Pisa, Italy.

[2] Department of Systems Medicine and Centre of Space Bio-medicine, University of Rome "Tor Vergata", Rome, Italy and with the Laboratory of Neuromotor Physiology, IRCCS Santa Lucia Foundation, Rome, Italy.

[3] Department of Advanced Robotics, Istituto Italiano di Tecnologia, via Morego, 30, 16163 Genova, Italy

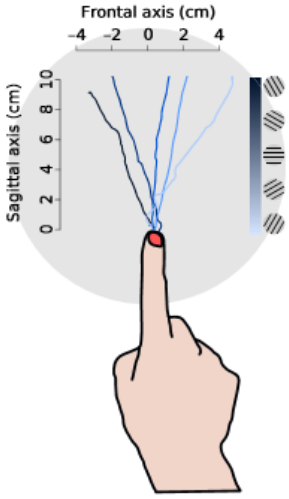

Figure 2: Average hand trajectories of a representative participant for the following ridges orientations (from the top): -60, -30, 0, 30, 60 deg. When the ridges were oriented of a negative angular value, the participant perceived a deviation towards right (negative value of θ), so the participant corrected the movement going toward left with respect to the mid-line of the plate (negative values of frontal axis)

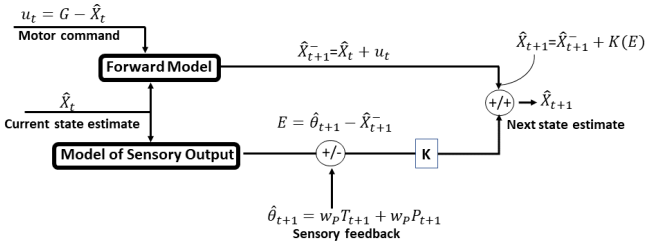

Figure 3: Scheme of the Kalman filter model.

[5], [6], [7]. In [8], we introduced an observer model for the integration of proprioception and touch in motor control. This framework is used to explain trajectory data for the reaching task performed on the ridged plate. The model accounted for the dynamic integration of proprioception, touch, and forward internal model. The model is schematized in Fig. 3. The motor command u_t is equal to the difference between G (the angular orientation of the desired trajectory with respect to the mid-line of the plate, in this case 0 deg) and the current state estimate of the hand angular position $\hat{X}_t$. The forward model predicts the following state of the angular displacement of the hand ($\hat{X}^-_{(t+1)}$); this internal estimate is compared to the sensory feedback ($\hat{\theta}_{t+1}$), generating the error term (E). In the task with the ridged plate, the sensory feedback is the perceived angular displacement of the hand, equal to the Bayesian integration of the muscular-skeletal proprioceptive ($P_{(t+1)}$) and tactile estimate ($T_{(t+1)}$), i.e., extrasomatic information. Motion direction

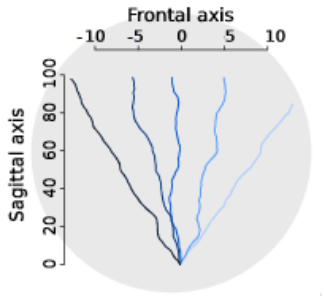

Figure 4: Kalman filter model: simulated results. The color code is the same as the one used for the experiment with the ridged plate (Fig.2)

resulting from extrasomatic information, which is perpendicular to the ridges orientation. This generates the observed bias in the trajectories. In the Bayesian framework, the integration arises from the weighted average of multiple independent cues [9]. The two weight terms of touch and proprioception, w_T and w_P, respectively, are assumed constant, with $w_P = 1 - w_T$. The error term E is weighted by the Kalman gain (K), and used to estimate the state of the system. The Kalman gain ($0 \leq K \leq 1$), at each time iteration, arises from the Bayesian combination of the variance of the forward model and the variance of the sensory feedback [10]:

$$K_t = \frac{\sigma^2_{\hat{x}_{t^-}}}{\sigma^2_{\hat{x}_{t^-}} + \sigma^2_{\hat{\theta}_t}}$$

According to the model, since $u_t = G - \hat{X}_t$, if a subject perceives an angular deviation, for example, toward left ($\hat{\theta} > 0$), this produces an update in the state estimate, triggering a correction movement to the right and vice-versa. We have showed that this model can reproduce the observed data, like the one of Fig. 2, and in particular the relationship between the angular orientation of the ridges of the plate and the observed trajectories. We have simulated the results of the experiment with $G = 0$ because the participants have to move straight and considering 75 simulated trials including five ridges orientations with 15 repetitions each. Each trial consisted of a simulated hand trajectory divided in 50 discrete steps of unitary length. We set $w_T = 0.15$ (with $w_P = 1 - w_T$). This is in accordance with previous studies that showed a smaller weight of touch compared with proprioception for the estimate of hand displacement [11], [12]. We set $\sigma^2_{\hat{\theta}_t}$ and $\sigma^2_{u_t}$ by trial and error to 50 and 1, respectively. The variance of the current state estimate was initialised to 10, and was updated in each iteration according to the equations of the Kalman filter. Results of the Kalman filter model are illustrated in Fig. 4. The model predicts the dependency of the motion direction upon the orientation of the ridged plate in a fashion similar to the experimental data. Then, we have shown that the effect of the tactile illusions still remain also when the participants performed the task on a rotating ridges plate [13]. The plate under the finger rotated with different angular velocities for each trial (-30, -15, 0, 15, 30 deg/s). The orientation of the ridges started from 0 deg and the duration of the rotation was 2 s, so at the end of the task the ridges orientation were : -60, -30, 0, 30, 60 deg respectively. Finally, we have shown that the kalman filter model can be also used to estimate the trajectories obtained in this last case, where the parameter that changes over time is the contribution of the tactile flow (T), which is perpendicular to the ridges at each time instant.

III. Conclusions

In this work, we have proposed a Kalman filter model to describe the illusion obtained on a steady ridged plate and the illusion obtained on a rotating ridged plate (called the *Turntable Illusion* [13]). The model allows to estimate the angular deviation of the hand, with respect to the mid-line of the ridged plate, at each time instant.These outcomes can pave the path towards next developments in human robot-machine interface design and control.

ACKNOWLEDGMENTS

This work is partially supported by the EU H2020 project "SOFTPRO: Synergy-based Open-source Foundations and Technologies for Prosthetics and RehabilitatiOn" (no. 688857), the Italian Ministry of Health (IRCCS Fondazione Santa Lucia, Ricerca Corrente), by the Italian Ministry of Education and Research (MIUR) in the framework of the CrossLab project (Departments of Excellence) and by Facebook Reality Lab (Facebook Inc.).

References

[1] M. Bianchi, A. Moscatelli, S. Ciotti, G. C. Bettelani, F. Fioretti, F. Lacquaniti, and A. Bicchi, "Tactile slip and hand displacement: Bending hand motion with tactile illusions," in *2017 IEEE World Haptics Conference (WHC)*. IEEE, 2017, pp. 96–100.

[2] G. C. Bettelani, A. Moscatelli, and M. Bianchi, "Towards a technology-based assessment of sensory-motor pathological states through tactile illusions," in *2018 7th IEEE International Conference on Biomedical Robotics and Biomechatronics (Biorob)*. IEEE, 2018, pp. 225–229.

[3] E. Battaglia, M. Bianchi, M. L. D'Angelo, M. D'Imperio, F. Cannella, E. P. Scilingo, and A. Bicchi, "A finite element model of tactile flow for softness perception," in *2015 37th Annual International Conference of the IEEE Engineering in Medicine and Biology Society (EMBC)*. IEEE, 2015, pp. 2430–2433.

[4] A. Bicchi, E. P. Scilingo, E. Ricciardi, and P. Pietrini, "Tactile flow explains haptic counterparts of common visual illusions," *Brain research bulletin*, vol. 75, no. 6, pp. 737–741, 2008.

[5] D. M. Wolpert, Z. Ghahramani, and M. I. Jordan, "An internal model for sensorimotor integration," *Science*, vol. 269, no. 5232, pp. 1880–1882, 1995.

[6] K. P. Körding and D. M. Wolpert, "Bayesian integration in sensorimotor learning," *Nature*, vol. 427, no. 6971, p. 244, 2004.

[7] J. Burge, M. O. Ernst, and M. S. Banks, "The statistical determinants of adaptation rate in human reaching," *Journal of vision*, vol. 8, no. 4, pp. 20–20, 2008.

[8] A. Moscatelli, M. Bianchi, S. Ciotti, G. Bettelani, C. Parise, F. Lacquaniti, and A. Bicchi, "Touch as an auxiliary proprioceptive cue for movement control," *Science advances*, vol. 5, no. 6, p. eaaw3121, 2019.

[9] M. O. Ernst and H. H. Bülthoff, "Merging the senses into a robust percept," *Trends in cognitive sciences*, vol. 8, no. 4, pp. 162–169, 2004.

[10] P. S. Maybeck, "Stochastic models, estimation, and control," *New York*, vol. 1, pp. 1–16, 1979.

[11] C. Blanchard, R. Roll, J. P. Roll, and A. Kavounoudias, "Combined contribution of tactile and proprioceptive feedback to hand movement perception," *Brain Research*, vol. 1382, pp. 219–229, 2011. [Online]. Available: http://dx.doi.org/10.1016/j.brainres.2011.01.066

[12] A. Moscatelli, M. Bianchi, A. Serio, A. Terekhov, V. Hayward, M. O. Ernst, and A. Bicchi, "The change in fingertip contact area as a novel proprioceptive cue," *Current Biology*, vol. 26, no. 9, pp. 1159–1163, 2016.

[13] G. C. Bettelani, A. Moscatelli, and M. Bianchi, "Contact with sliding over a rotating ridged surface:the turntable illusion," in *2019 IEEE World Haptics Conference (WHC)*. IEEE, 2019, In press.

An approach to convey proprioception and force feedback in subjects with limb loss

Federica Barontini[1,2,3], Simone Fani[1,2,3], Giorgio Grioli[3], Manuel G. Catalano[3], Matteo Bianchi[1,2], and Antonio Bicchi[1,3]

***Abstract*— Hands are our preeminent organ to interact with and explore the external environment. People with hand loss e.g. transradial amputees cannot receive the crucial information from the environment, as they would naturally perceive with their intact hands. It is not hence surprising that a lot of effort has been devoted to find alternative solutions to convey touch-related cues such tangential force, grasping force, pressure relying on haptic devices, to be applied at different body locations. In this extended abstract we presented a re-designed mechatronic system to convey information to limb loss subjects, using a wearable fabric-based device (Clenching Upper-Limb Force Feedback, CUFF). This device provides distributed mechano-tactile stimulation on the users arm skin, in term of pressure and stretch cues. The provided feedback is related to grasping forces and proprioceptive information on the prosthetic hand aperture. A complete characterization of the system and psycho-physical experiments, which investigate the usability of the device to effectively convey proprioception and grasping force, are presented.**

I. INTRODUCTION

Touch represents a powerful information generator. Not surprisingly, a lot of effort has been devoted to design human-robot interfaces, to convey haptic cues to humans in an effective manner, especially for limb-loss subjects where the natural action-perception loop is interrupted [1]. One possible solution is through Wearable Haptic Systems (WHS), mechatronic devices capable to convey information to the users, yet preserving the wearability and the usage simplicity [2]. Most of the devices presented in literature so far mainly act only at the finger level see [3], or they are not able to simultaneously deliver tangential or normal force information at the arm or forearm level. In this work we present a novel approach to convey both proprioceptive and force feedback using a wearable haptic device at the arm level. In particular we described a thorough characterization of the Cleching Upper-limb Force Feedback (CUFF) device, for delivering information on the estimated grasping force and the level of aperture (proprioception) of a soft prosthetic hand. Preliminar psycho-physical experiments, with able-bodied participants, were conducted to identify the perceptual workspace that the device can act on, to elicit pressure and tangential skin stretch perception.

[1] Research Center "E.Piaggio", University of Pisa, Largo L. Lazzarino 1, 56126, Pisa, Italy,
matteo.bianchi@centropiaggio.unipi.it

[2] Dipartimento di Ingegneria dell'Informazione, University of Pisa, Largo L. Lazzarino 1, 56126, Pisa, Italy.

[3]Fondazione Istituto Italiano di Tecnologia, via Morego 30, 16163, Genova, Italy.

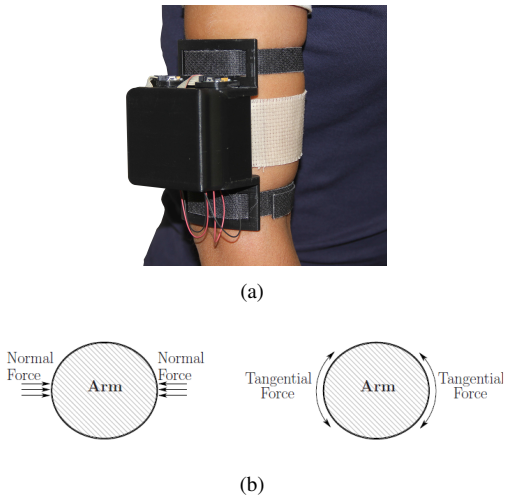

Fig. 1. Device overview (a) and working modes of the CUFF (b)

II. THE WEARABLE HAPTIC DEVICE

We used a redesigned version of the Clenching Upper-Limb Force Feedback (CUFF wearable device for distributed mechano-tactile stimulation of normal and tangential skin forces (see Fig:1) presented in [4]. The CUFF was thought to be used in conjunction with a soft prosthetic hand SoftHand Pro, which is endowed with a single actuator but it can adapt to different items.

Briefly, the CUFF consists of two DC motors attached to a band, or cuff, worn around the user's arm. When the motors spin in opposite directions, they tighten or loosen the band on the arm, thus conveying a normal force, related to the estimated grasping force. On the contrary, when the motors spin in the same direction, the fabric can slide around the arm, thus conveying tangential force cues and, hence, directional information. This cue can be related to the level of the aperture of the hand (proprioception). The two stimulation modalities can be used to deliver both grasping force and proprioceptive information.

The CUFF device is endowed with a custom made electronic board (PSoC-based electronic board with RS485 communication protocol) [5], which enables to control the position of the motors, based on the readings of two magnetic encoders AS4550, one for each motor. The actuation unit is powered by a battery pack of 12 Volt.

III. CHARACTERIZATION OF THE SYSTEM

We performed a characterization of the CUFF. The goals of the characterization were to obtain a relation between the position of the motors of the device (with respect to a variable zero position) and the normal force exerted by the fabric belt on the subject's arm, and also to compare different control techniques implemented for the CUFF device. A 3-axis force sensor, the ATI Gamma, was used to measure the normal force exerted by the CUFF. To measure the normal force exerted by the device, we designed a structure, like a cylinder, to adapt the shape of the sensor to the device. Five cylinders with different radii (80, 85, 90, 100 and 115mm), which approximate different human arm dimensions, were printed with a 3D printer in Rapid Prototyping material (ABS). As first analysis we performed a characterization of the device using the current control, but the results obtained shown a too wide hysteresis effect between the current absorbed by the motors and the normal force elicited. Therefore, we chose to use the position and current control mode for this characterization and for all the experiments. The position and current control mode, consisted of a double loop composed of an external position loop and an internal current loop. The position controller generates the current reference and the current controller generates the PWM output, which feeds the motor to produces the movement. The characterization was performed using a series of step of closing-opening movements of the CUFF, around the designed cylinders. The motors rotated in opposite directions, in order to pull the fabric without generating side-scrolling movements. Ten repetions per radius were performed. The maximum commanded position was 800 tics (corresponding to 17°) and the movement was performed such that this position was reached in 50 seconds. The results shown that the maximum reachable position corresponding to the maximum current absorption, produced an average a force of 25 N on the sensor.

IV. PSYCOPHISICAL TESTS

We used standard psychophysical methods to estimate user's ability to discriminate the normal force and the tangential displacement delivered with the CUFF. Eleven right-handed healthy participants (7 female, Age mean ± 26.64) gave their informed consent to partecipate to the experiment.

A. Tangential Displacement Perception

Participants were comfortable seated, wearing the CUFF on their arm, headphones with white noise to prevent auditory cues and glasses to cover the sight. We used the method of the constant stimuli, where each trial consisted of a reference stimulus (RS) and a comparison stimulus (CS), presented in a pseudo random order. The displacement was equal to 17.91 mm in the RS, and was pseudo-randomly chosen among five discrete and equally space values (5.97, 11.94, 17.91, 23.88, and 29.85 mm) in the CS. Participants were asked to indicate which stimulus interval the tangential displacement was perceived as larger. The inter-stimulus interval was 2 s. In two separate blocks, each of 100 trials, the direction of tangential motion was either rightward or leftward, and the order of the two blocks was counterbalanced. We modeled the responses of each voluteer using the psychometric function, and we extended it to the whole pool of participants by means of a Generalized Linear Mixed Model (GLMM) [6]. For each experimental condition, we estimated the Just Noticeable Different (JND), i.e. the amount of stimulus change to produce a noticeable perceptual change, and the Point of Subjective Equality (PSE), i.e. the stimulus value yielding a response probability of 0.5. The JND provided an estimate of the precision of the response; the PSE estimated the accuracy of the response. The results showed that the difference in JND between the two conditions was not statistically significant, while the PSE revealed a very accurate response for rightward and leftward moving stimuli.

B. Normal Force Perception

The experimental setup and procedure was the same as for the tangential displacement task. Participants experienced paired stimuli and they were asked to indicate which stimulus in the pair produced a higher normal force. The force values were equal to 9 N in the RS, and was pseudo randomly chosen among five stimuli (3, 6, 9, 12, 15 N) in CS. The stimulus duration was 1 s, while the inter-stimulus interval was 2 s. Data were analyzed as for the tangential task. Also in this case the PSE demonstrated that the response was accurate and precise.

V. CONCLUSIONS AND FUTURE WORKS

In this work we presented a miniaturization of the first design of the CUFF, with the performed characterization. We observed that the stimuli generated by the new device were well perceived by the users wearing it on the upper arm, both in normal force and tangential sliding modes, with no difference between the two directions of sliding. Even if the experiments were performed only on able bodied subjects, the obtained results are encouraging. Future works will involve explorative experiments, focusing more on the prosthetic application side, with able bodied and amputees participants.

REFERENCES

[1] D. Katz and L. Krueger, *The World of Touch*. L. Erlbaum, 1989. [Online]. Available: https://books.google.it/books?id=49Vtnp2k1MEC

[2] B. Hannaford and A. M. Okamura, "Haptics," *Springer Handbook of Robotics*, pp. 719–739, 2008.

[3] D. Leonardis, M. Solazzi, I. Bortone, and A. Frisoli, "A wearable fingertip haptic device with 3 dof asymmetric 3-rsr kinematics," in *2015 IEEE World Haptics Conference (WHC)*, June 2015, pp. 388–393.

[4] S. Casini, M. Morvidoni, M. Bianchi, M. Catalano, G. Grioli, and A. Bicchi, "Design and realization of the cuff - clenching upper-limb force feedback wearable device for distributed mechano-tactile stimulation of normal and tangential skin forces," in *Intelligent Robots and Systems (IROS), 2015 IEEE/RSJ International Conference on*, Sept 2015, pp. 1186–1193.

[5] Natural machine motion initiative. [Online]. Available: https://www.naturalmachinemotioninitiative.com/

[6] A. Moscatelli, M. Mezzetti, and F. Lacquaniti, "Modeling psychophysical data at the population-level: the generalized linear mixed model," *Journal of vision*, vol. 12, no. 11, pp. 26–26, 2012.

Functional impairment and muscular activity analysis of upper limb in patients with multiple sclerosis: a cross-sectional study

Valè N[1], Gandolfi M[1], Dimitrova E[1], Mazzoleni S[2], Battini E[2], Benedetti MD[1], Gajofatto A[1], Ferraro F[3], Castelli M[4], Camin M[4], Filippetti M[1], Corradi J[1], De Paoli C[1], Picelli A[1], Smania N[1]

***Abstract*—This study aims to investigate UL deficits in a cohort of people with Multiple Sclerosis (MS). Moreover, muscle activity of 6 upper limb muscles has been recorded during a functional task of reaching and grasping. 42 Subjects with MS have been included (EDSS=2-8) and stratified according to neurological disability in 3 groups: moderate (EDSS 4.5-6; n=15); severe (EDSS 6.5-8; n=17). Surface electromyography has been used to analyze muscle activation during a reaching and grasping task (ARAT grasp section). Results showed a progressive decreasing in upper limb capacity and function. Data on clinical assessment are associated with decreasing in muscle activity modularity in distal upper limb muscles.**

I. Introduction

Multiple sclerosis (MS) is the most common non-traumatic cause of neurologic disability in young adults, [1][2]. Walking ability is often the target of rehabilitation approaches; however, restriction in arm function has a remarkable impact on the MS patient's ability to perform activities of daily living and on quality of life perception [3]. The impairment of the function and activity of the upper limb (UL) represent one of the emerging research areas in patients with Multiple Sclerosis (PwMS). UL dysfunction affects quality of life and independence on a ICF point of view. Several underlined the crucial role of the hand dexterity and its strong association with participation restriction and ADL performance [4][5][6] Moreover, severe impairment in hand dexterity has been reported to reflect plasticity maladaptation [1]. Although the literature emphasizes the relevance of rehabilitation in decreasing these impairments and improving quality of life, to date, further research is needed to identify the nature of UL neuromuscolar dysfunction [7].

Primary aim was to evaluate UL deficits in a PwMS cohort stratified by neurological involvement according to the EDSS scale. Secondary aim was to investigate muscle activation using surface electromyography (sEMG) during a standardized motor task.

II. Material and Methods

A cross-sectional study was conducted on 42 PwMS (mean age 51±11 years; EDSS = 2-8) with functional deficits of UL. Inclusion criteria: EDSS < 9, Mini Mental State Examination > 24, Modified Ashworth Scale UL < 3, Nine Hole Peg Test 30s-300s. The patients were stratified in three groups: "mild" (EDSS 2-4; n=10); "moderate" (EDSS 4.5-6; n=15); "severe" (EDSS 6.5-8; n=17). Primary outcome: Action Research Arm test (ARAT). Secondary outcomes: Nine-Hole Peg Test (NHPT); Motricity Index (MI); Fugl-Meyer Assessment (FMA); Motor Activity Log (MAL); Visual Analogue Scale for Fatigue (VAS-F); Assessment of Life Habits (LIFE-H); MS Quality of Life-54 (MSQOL-54); evaluation of muscle activity with poly-EMGds. The sEMG acquisition was performed in 6 muscles of the UL with greater FI (anterior/posterior deltoid, biceps/triceps brachial, flexor/extensor carpi radials) during a standardized task (Grasp section of ARAT) repeated for 3 times.

Clinical data were analyzed with non-parametric tests (SPSS ver.23). For the multiple comparisons, the Bonferroni correction was applied ($p \leq 0.016$). Poly-EMGs signal was processed using routines developed in the Matlab environment (Mathworks Inc USA) and was normalized with respect to the EMG signal detected in the rest and MVC conditions.

III. Results

The three groups differed from each other about the age ($p=0.028$), manual dexterity ($p=0.042$), FMA scale score ($p=0.025$), amount of limb use ($p=0.012$), quality of

The study was supported by a FISM (Fondazione Italiana Sclerosi Multipla onlus) grant no. 2013/R/24. Some data of the present work have been previously presented at WCPT Congress 2019.

V.N., M.G., D.E., B.M.D., G.A., F.M., C.J., DP. C., P.A., S.N.. are with the Department of Neurosciences, Biomedicine and Movement Sciences of the University if Verona, Verona, Italy. (corresponding author to provide e-mail: nicola.vale@univr.it).

M.S., and B.E., are with the Biorobotics Institute, Scuola Superiore Sant'Anna di Pisa, Pontedera, Italy.

F.F. is with the Azienda Sociosanitaria di Mantova, Department of Neuroscience, Mantua, Italy.

Castelli M., Camin M., are with the ATSM Centro Franca Martini, Trento, Italy.

movement (p=0.004) and perception in performing motor tasks of daily life both in terms of difficulty (p< 0.001) and satisfaction (p=0.007). Post-hoc comparison between the three groups showed that the "mild" and "moderate" groups

TABLE I

		MS subgroups			p-value
		Group 1	Group 2	Group 3	
	Total (n=42)	Mild EDSS (2-4) (n=10)	Moderate EDSS (4.5-6) (n=15)	Severe EDSS (6.5-8) (n=17)	
Gender (F/M)	25/16	6/4	9/6	9/8	n.s.
Age (years)	51.2±11.0	42.6±13.5	52.0±7.7	55.5±9.4	0.05*
EDSS	6 (4.25-6.5)	3.75 (3.37-4)	6 (5.5-6)	7. (6.5-8)	<0.001*
Hand dominance (R/L/A)	34/8/0	7/3/0	10/5/0	17/0/0	n.s.
Disease duration (years)	14.2±8.7	10.7±13.1	19.5±17.1	5.8±14.2	n.s.
Type of MS (PP/RP/RR/SP)	2/2/22/16	0/1/8/1	1/0/11/3	1/1/3/12	0.05*
Visual Impairment (yes/no)	2/40	0/10	1/15	1/17	n.s.

Tab. 1 Clinical and demographic characteristic of the sample

did not differ statistically significantly in the different outcome measures. The "mild" group differed from the "severe" group in terms of age (p=0.016), UL function evaluated by FMA (p=0.016) and the use of UL as quantity (p=0.009) as in quality (p=0.003). Furthermore, the "mild" group and the "severe" group did not differ in manual dexterity evaluated at the NHPT (p=0.022). The "moderate" and "severe" groups showed no significant differences both in terms of quantity (p=0.024) and quality (p=0.025) of UL use.

Preliminary analysis of sEMG data showed a progressive lower modulation of muscle activity in the patients of the "moderate" and "severe" groups.

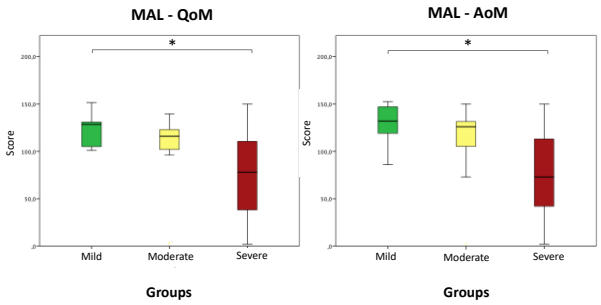

Fig. 1. Motor Activity Log results. QoM: Quality of Movement subscore; AoM: Amount of Movment subscore; *: between-group comparison p<0.05.

IV. DISCUSSION

The present study investigated UL performance in a cohort of patients with MS stratified according to neurological disability. Although no significant differences between groups were found on primary outcome and hand dexterity, a progressive UL function worsening was measured at FMA. Data analysis showed that patients in the severe groups presented significantly less use of UL in domestic environment compared to group 1 and 2. This suggested that UL disuse may occur also in early stages of disability and can be measured even when functional and activity impairment are not measured. Moreover, sEMG analysis showed progressive decreasing in muscles activity modularity especially in the forearm muscles. These findings are in keeping with previous results of a Pellegrino et al. pilot study [8]. In this context, the muscular impairment might represent a measure of subclinical UL impairment.

V. CONCLUSION

This study shows as one of the first disorders is the misuse of the limb and providing interesting insights into the pathophysiology of UL dysfunctions in PwMS. These results showed different neuromuscolar dysfunction in PwMS related to neurological impairment. The present findings are relevant to identify different rehabilitation strategies based on the level of the impairment of the UL.

REFERENCES

[1] Tomassini V, Matthews PM, Thompson AJ, Fuglø D, Geurts JJ, Johansen-Berg H et al. Neuroplasticity and functional recovery in multiple sclerosis. Nat Rev Neurol. (2012) 8:635-46. doi: 10.1038/nrneurol.2012.179W.

[2] Thompson AJ, Baranzini SE, Geurts J, Hemmer B, Ciccarelli O. Multiple sclerosis. Lancet. (2018) 391:1622-1636. doi: 10.1016/S0140-6736(18)30481-1H.

[3] Mokkink LB, Knol DL, van der Linden FH, Sonder JM, D'hooghe M, Uitdehaag BMJ. The Arm Function in Multiple Sclerosis Questionnaire (AMSQ): development and validation of a new tool using IRT methods. Disabil Rehabil. (2015) 37:2445-2451. doi: 10.3109/09638288.2015.1027005

[4] Bertoni R, Lamers I, Chen CC, Feys P, Cattaneo D. Unilateral and bilateral upper limb dysfunction at body functions, activity and participation levels in people with multiple sclerosis. Mult Scler. (2015) 21:1566-74. doi: 10.1177/1352458514567553E.

[5] Lamers I, Cattaneo D, Chen CC, Bertoni R, Van Wijmeersch B, Feys P. Associations of upper limb disability measures on different levels of the International Classification of Functioning, Disability and Health in people with multiple sclerosis. Phys Ther. (2015) 95:65-75. doi: 10.2522/ptj.20130588.

[6] Cattaneo D, Lamers I, Bertoni R, Feys P, Jonsdottir J. Participation Restriction in People With Multiple Sclerosis: Prevalence and Correlations With Cognitive, Walking, Balance, and Upper Limb Impairments. Arch Phys Med Rehabil. (2017) 98:1308-1315. doi: 10.1016/j.apmr.2017.02.015M.

[7] Lamers I., Maris A., Severijns D., Dielkens W., Geurts S., Van Wijmeersch B. et al. Upper Limb Rehabilitation in People With Multiple Sclerosis: A Systematic Review. Neurorehabil Neural Repair. (2016) 30: 773-793. doi:10.1177/1545968315624785.

[8] Pellegrino L., Stranieri G., Tiragallo E., Tacchino A., Brichetto G., Coscia M. et al. Analysis of upper limb movement in Multiple Sclerosis subjects during common daily actions. In: Engineering in Medicine and Biology Society (EMBC), Procedings of the 37th Annual International Conference of the IEEE, Milan, Italy, 2015 Aug 25–29, paper no. 15585597. IEEE. doi: 10.1109/EMBC.2015.7319995

Analysis of Compensatory Movements Using a Supernumerary Robotic Hand for Upper Limb Assistance

Martina Rossero [1,2], Andrea S. Ciullo[1,2], Giorgio Grioli[1], Manuel G. Catalano[1], and Antonio Bicchi[1,2] .

***Abstract*— This study investigates compensatory movements exploited by users of a supernumerary robotic hand for upper limb assistance. Results demonstrated that elbow and shoulder ranges of motion are lower during the execution with the robotic system with respect to the free execution but these reduced movements are compensated by the larger ranges of motion of the trunk and of the head. For what concerns, instead, the accuracy and the efficiency indices used to compare the hand trajectories exploited, the values obtained are quite low, showing a higher variability between subjects. The muscles activation was very similar for the two executions. From this study resulted that the system doesn't affect the subject movements and his capability to perform grasping movement.**

I. INTRODUCTION

The musculoskeletal architecture of the upper body contains redundant degrees of freedom so the central nervous system can select different equivalent motor strategies and associated inter-joint coordination patterns to perform different type of tasks [1]. When an upper limb is impaired, for example after a stroke, or replaced with a prosthetic device after an amputation, patients may develop alternative grasping strategies by using this redundancy [2]-[3]. Since it has been demonstrated that some of them can be detrimental [4], it is important to evaluate their entity. In recent years, many robotic devices have been developed to help stroke patients. Nowadays, a new trend is emerging: the Supernumerary Robotics Limbs (SRL). They consist of additional artificial limbs, hands or fingers, that can perform tasks in close coordination with a subject wearing them. A notable example is the sixth finger device [5], which has been successfully tested with stroke patients. The aim of this study is to evaluate the compensatory movements performed by a subject using a supernumerary robotic hand for upper limb assistance, the SoftHand X (SHX) system. It is a robotic system consisting of an anthropomorphic artificial hand and a passive gravity compensator. An input interface, connected to the SHX is used by the subject to control the robotic hand.

II. MATERIAL AND METHODS

A. Tasks

11 healthy subjects were asked to perform a modified version of the Action Research Arm Test (mARAT) that is a clinical hand assessment test, involving the manipulation of objects differing in size, weight and shape.

[1] Italian Institute of Technology (IIT), Genoa, Italy.
[2] Bioengineering and Robotics Research Center "E. Piaggio" of University of Pisa, Pisa, Italy

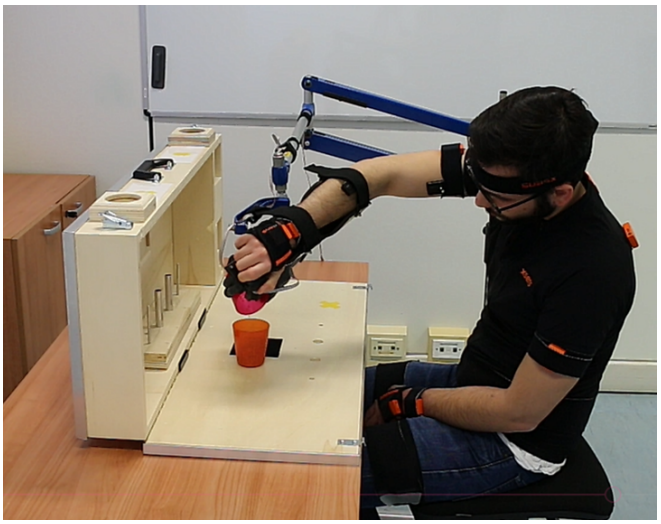

Fig. 1. Example of head and trunk compensatory movements performed by a subject during the execution of a task of the ARAT test (pouring task).

B. Data acquisition

The Xsens MVN system was used to obtain kinematic data recorded with a sample frequency of 60 Hz. Data acquired were body segment position and upper body joints angles (shoulder, elbow, wrist, trunk and neck). The Trigno Delsys wireless system was used to record the electromyographic (EMG) signals of the muscles of the upper arm (trapezius, lateral deltoid, biceps, triceps lateral head and ulnar flexor and extensor of the wrist) with a sample frequency of 2 kHz. Subjects executed the tasks at first with their own hand, then using the SoftHand X system placed in two different configurations. Such positions are the result of previous studies on the manipulability and workspace of the system [6]. The first position has the SoftHand X in front of the natural hand, aligned with user's arm, the second configuration has the robotic hand below the natural one. Before the acquisition, all the subjects had some minutes of training and during configuration changes they were given a few minutes to rest.

C. Data analysis

The Range of Motion (RoM) of the joints was calculated as the difference between the maximum and the minimum measured angles, as reported in similar studies [2]-[3].
Movements considered are the abduction/adduction, the flexion/extension and the rotation of the right shoulder, right wrist, head and trunk and the flexion/extension of the right

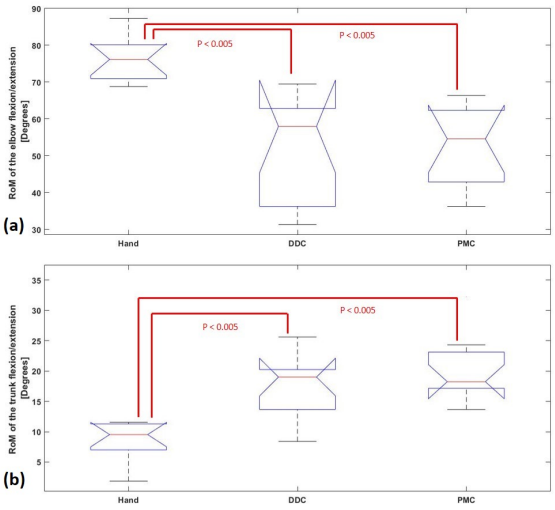

Fig. 2. Example of (a) decreasing of the RoM of the elbow flexion/extension and of (b) increasing of the RoM of the trunk flexion/extension during the execution of a task without and with the SHX system.

elbow. An accuracy index and an efficiency index have been computed, as described in [7]. The first is proportional to the mean distance and to the correlation between the hand trajectories exploited with and without the robotic system. The second compares the path length of the hand trajectories. To evaluate the muscles activation, the RMS value was calculated from the filtered, rectified and normalized EMG signals.

III. Results and Discussion

For what concerns the wrist, the differences obtained by subtracting the RoM obtained with the robotic hand to the ones obtained with the natural hand are high (reaching more than 30 degrees for some tasks) and positive. By consequence, the RoM during the execution with the natural hand was much higher. Considering the shoulder joint, in simple tasks, such as the lifting of objects, the RoM are similar or even lower during the execution with the SHX system while, in tasks requiring a higher precision and specially in the pouring task, the RoM was higher. For what concerns the elbow flexion/extension movement the RoM obtained from the execution with the robotic hand is always lower (as shown in the example of Figure 2(a)) except in the case of the pouring task. This is in line with the fact that, as previously said, this task also required a bigger movement of the shoulder. The biggest differences are reported for the trunk and head movements. In fact, during the execution with the robotic hand the subject exploited more these joints movements. This is due to the fact that, having the arm more constrained by the SHX system, subjects need these compensatory movements to accomplish the tasks. Moreover, this can also be attributed to the fact that the robotic hand tends to hide the object. An example of trunk RoM increasing is shown in Figure 2(b). For what concerns the accuracy and efficiency index, the values obtained during the execution of the test with the natural hand are quite low, showing a big variability in the trajectories exploited by different subjects. This can explain the very low values obtained for the two configurations of the SHX system. In fact they can be caused not only by the encumbrance of the robotic system but also by the difference in the strategy and trajectory used.

From the EMG signal analysis, the values of the RMS resulted very similar between the task execution with and without the SHX system. This can be due to the fact that all the tasks proposed were very fast and all the items had a light weight so in both cases, none of the subjects experienced evident level of fatigue. It was also noticed that the muscle activity resulting from the execution with the natural hand shows always a relaxing period between the different repetitions while during the execution with the SHX system the muscle activity was present also in this phase. This can be due to the encumbrance of the human-arm interface pushing the subject to contract the muscles to maintain the position.

IV. Conclusion

In this study, it has been demonstrated that, the SHX system can be useful to reduce the stress on the wrist, elbow and shoulder joints, since the RoM exploited decreased. This is caused by the effect of the gravity compensator, helping the subject to move the arm, and by the position of the robotic hand, reducing the distance to the objects. To compensate these reduced movements, trunk and head RoM increased. However, since a stroke patient tends to have pain to the shoulder and difficulties in the lifting of his/her arm, these results demonstrate that this device could be really useful in the assistance of these patients. Moreover, as resulted from the EMG signals analysis, the muscles activity was not so different during the use of the system, thus demonstrating that this device is not detrimental from the point of view of the fatigue. A limit of this study is the fact that only healthy subjects were analysed so, for further investigation, the same experiments could be conducted with post-stroke patients.

References

[1] F. M. Ivaldi, P. Morasso, and R. Zaccaria, "Kinematic networks," *Biological cybernetics*, vol. 60, no. 1, pp. 1–16, 1988.

[2] S. L. Carey, M. J. Highsmith, M. E. Maitland, and R. V. Dubey, "Compensatory movements of transradial prosthesis users during common tasks," *Clinical Biomechanics*, vol. 23, no. 9, pp. 1128–1135, 2008.

[3] M. Cirstea and M. F. Levin, "Compensatory strategies for reaching in stroke," *Brain*, vol. 123, no. 5, pp. 940–953, 2000.

[4] L. Ada, C. Canning, J. Carr, S. Kilbreath, and R. Shepherd, "Task-specific training of reaching and manipulation," in *Advances in psychology*. Elsevier, 1994, vol. 105, pp. 239–265.

[5] I. Hussain, G. Salvietti, G. Spagnoletti, and D. Prattichizzo, "The soft-sixthfinger: a wearable emg controlled robotic extra-finger for grasp compensation in chronic stroke patients," *IEEE Robotics and Automation Letters*, vol. 1, no. 2, pp. 1000–1006, 2016.

[6] A. S. Ciullo, F. Felici, M. G. Catalano, G. Grioli, A. Ajoudani, and A. Bicchi, "Analytical and experimental analysis for position optimization of a grasp assistance supernumerary robotic hand," *IEEE Robotics and Automation Letters*, vol. 3, no. 4, pp. 4305–4312, 2018.

[7] A. de los Reyes-Guzmán, I. Dimbwadyo-Terrer, S. Pérez-Nombela, F. Monasterio-Huelin, D. Torricelli, J. L. Pons, and A. Gil-Agudo, "Novel kinematic indices for quantifying upper limb ability and dexterity after cervical spinal cord injury," *Medical & biological engineering & computing*, vol. 55, no. 5, pp. 833–844, 2017.

Simultaneous and Proportional Decoding of Stiffness and Position Intentions from Two sEMG Channels for Upper Limb Prosthetics

P. Capsi-Morales[1,2], G. Grioli[2], M. G. Catalano[2], C. Piazza[1] and A. Bicchi[1,2]

I. INTRODUCTION

Among functional hand prostheses, the role of myoelectric hands is particularly important as users operate the device directly with their muscle signals. Humans continuously adapt the stiffness and the force of their limbs to match with the environmental requirements through the use of antagonistic muscle coactivation. However, this aspect is not fully reflected in current direct controlled prosthetic aids, neither its investigation is fully exploited in literature, both from the control [1] and mechatronics point of view. We introduce a simultaneous and proportional control output, based on cocontraction, combined within an integral position control framework, that reduces the fatigue experienced by the users. The primary objective is to exploit cocontraction for a useful and intuitive increase of direct control robustness, a better decoding of patient's intentions and to enlarge prosthesis dexterity (see Fig. 1).

We explored the utility of variable stiffness control in prosthetic hands while preforming activities of daily living and physical social interactions. Artificial limbs are very valuable to restore some of the capabilities lost after an amputation. However, there is still a sharp separation between available functional devices and the real needs of prosthetic users [2]. Social interaction and safety are aspects that cannot be underestimated in prosthetics, especially in upper limb, due to the inherent interaction of the artificial hand with, not only the user, but also the rest of the world. Already in 1983, Hogan [3] suggested impedance control as the preferred paradigm for controlling prostheses, as it would provide the amputee with an essential component of the natural adaptative capability of humans, despite the severe sensory loss. Moreover, behavioural studies of postural limb control show that humans modulate joint stiffness to minimize the perturbing effects of external loads [4] and it was proven to benefit limb stability and movement accuracy [5]. We postulate that the improvement of such social capabilities, which promote bionic interaction, would also favour hand prostheses acceptance.

*This research has received funding from the European Union's Horizon 2020 Research, Innovation Programme under Grant Agreement No.688857 (SoftPro) and ERC programme under the Grant Agreement No.810346 (Natural Bionics). The content of this publication is the sole responsibility of the authors. The European Commission or its services cannot be held responsible for any use that may be made of the information it contains.

[1]Centro "E. Piaggio" and Dipartimento di Ingegneria Informatica, University of Pisa, Largo Lucio Lazzarino 1, 56127 Pisa, Italy.

[2]Istituto Italiano di Tecnologia, Via Morego 30, 16163, Genoa

Correspond to: patri.capsi@gmail.com

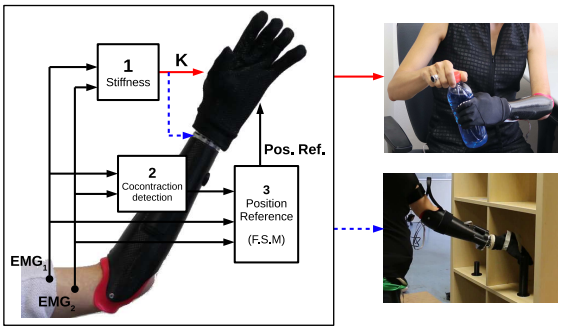

Fig. 1. Block diagram of the proposed algorithm: decoding of stiffness and position references from a pair of sEMG. The extra control output (stiffness) could be applied to control the compliance of the grasp (red line) or the stiffness of a lockable wrist (blue dashed line) to increase the prosthesis dexterity.

II. DECODING OF STIFFNESS & POSITION

We define stiffness K (see block diagram in Fig. 1) with the simplest way to estimate cocontraction (used e.g. in [6]). K is proportional to the total activation of subject's muscles, which can either be due to involuntary reaction to external disturbances, voluntary cocontraction, or reciprocal muscle activation. Due to the use of integral control of hand's position, the level of the extensor muscle contraction is almost zero when closing, and the opposite happens when opening. Therefore, we define cocontraction detection CD as in

$$CD = \begin{cases} 0 & \text{if } \min(K_1 EMG_1, K_2 EMG_2) < Th_{CD} \\ 1 & \text{otherwise,} \end{cases} \quad (1)$$

where Th_{CD} is a suitable threshold value. Consequently, CD is considerable only when cocontraction is intended, as both sEMG have a high level of activation.

A Finite State Machine (see Fig. 2) is used to discriminate the user's intention to modify RC (opening or closing the hand) or to hold it still. Previously, pure cocontraction phenomena, unless perfectly symmetrical and synchronized (which never happens in practise), would be interpreted as either open or close commands, depending on which of the two EMG signals is observed overcoming its threshold first. Accordingly, more robust conditions are applied considering not just the two sEMG values, but also CD as inputs.

III. GRASP COMPLIANCE

The proposed method was implemented on a soft underactuated hand device, the SoftHand Pro [7]. To the best

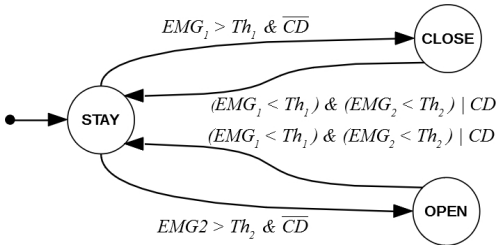

Fig. 2. Finite State Machine used to refine integral position reference of the hand. The starting state is *STAY*. The conditions let the system jump from one state to another.

knowledge of the authors, this is the first experimental validation of impedance control in prosthetics hands preformed by an amputee. The user rated the system usability (SUS) [8] after performing a set of tasks, which included one- and two-handed object manipulation, self interaction, and social interaction with 12 able-bodied volunteers, without having any information about the control used on it. Volunteers reactions were also collected and analysed as they rated quality, human-likeness, safety and comfort on a likert scale. Three examples of the tasks performed are presented in Fig. 3. The study explores the effects of variable stiffness control compared to strategies with a constant stiffness value.

The results present evidences that the different strategies implemented influence the perception of the subjects. Moreover, we can also infer the difficulties on task execution from the experienced performance differences. The user started preferring the high stiffness control (HS) due to its reactivity, which feels more natural and personal as the hand responds faster to commands. However, this changed over the course of the experiment when the possibility of causing discomfort to people when interacting, due to an excessive squeezing, arose. The user also underlined the lack of confidence and difficulties to command the hand when using the low constant stiffness controller (LS), because of the opposite reason, i.e. lack of reactivity. Finally, proportional control (PS) was perceived as the easiest system to use and learn during the whole test, in accordance with the fact that it is designed with different stiffness requirements and adapts to situations. The user was able to understand the differences in performance between cases and diverse elicited sensations. About the opinion and perception of the secondary subjects, we found statistical significance looking at "human-likeness" and "comfort" aspects, where high and low constant stiffness are significantly different. Nevertheless, results seem to

(a) (b) (c)

Fig. 3. Bionic interaction experiments: The prosthetic user hand-shakes (a), walks holding hands (b) with another subject and (c) self-interact.

suggest a general preference of low stiffness in all factors. In addition, we noted that in all factors, the proportional control (PS) rates between HS and LS, which highlights the differences (although not significant) between HS and PS. To sum up, encouraging results evidence that variable stiffness could be a possible compromise between modalities that just favour either firm control or delicate interaction. This insight suggests to extend this pilot study by including multiple prosthetic subjects and different robotic hands.

IV. Antropomorphic lockable wrist

The same principle is applied to control the stiffness of a passive wrist, designed on purpose. We present a 3 DoFs compliant wrist, lockable in any configuration using only one motor, that could improve the prosthesis functionality. Thanks to the use of muscle coactivation, it is possible to easily control wrist stiffness gradient and improve the grasp naturalness and the control intuitiveness of the hand-wrist system. Preliminary results suggest that using a simple control strategy and with an anthropomorphic design (see Fig. 4), it is possible decide hand orientation for those situations where the arm pre-grasping configuration is fundamental, decreasing the amount of compensatory movements as well.

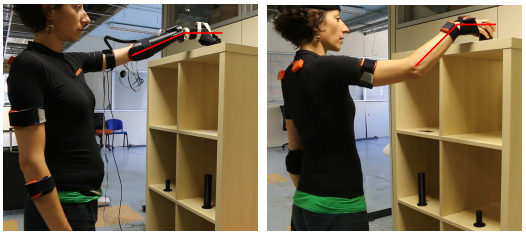

(a) Lockable wrist (b) Intact wrist

Fig. 4. Example of the natural wrist configuration using the novel prosthetic wrist compared to user's intact arm.

References

[1] A. E. Schultz and T. A. Kuiken, "Neural interfaces for control of upper limb prostheses: the state of the art and future possibilities," *PM&R*, vol. 3, no. 1, pp. 55–67, 2011.

[2] D. J. Atkins, D. C. Heard, and W. H. Donovan, "Epidemiologic overview of individuals with upper-limb loss and their reported research priorities," *JPO: Journal of Prosthetics and Orthotics*, vol. 8, no. 1, pp. 2–11, 1996.

[3] N. Hogan, "Prostheses should have adaptively controllable impedance," in *Control Aspects of Prosthetics and Orthotics*. Elsevier, 1983, pp. 155–162.

[4] M. L. Latash, "Independent control of joint stiffness in the framework of the equilibrium-point hypothesis," *Biological cybernetics*, vol. 67, no. 4, pp. 377–384, 1992.

[5] P. L. Gribble, L. I. Mullin, N. Cothros, and A. Mattar, "Role of cocontraction in arm movement accuracy," *Journal of neurophysiology*, vol. 89, no. 5, pp. 2396–2405, 2003.

[6] A. Ajoudani, S. B. Godfrey, M. Catalano, G. Grioli, N. G. Tsagarakis, and A. Bicchi, "Teleimpedance control of a synergy-driven anthropomorphic hand," in *Intelligent Robots and Systems (IROS), 2013 IEEE/RSJ International Conference on*. IEEE, 2013, pp. 1985–1991.

[7] S. B. Godfrey, K. D. Zhao, A. Theuer, M. G. Catalano, M. Bianchi, R. Breighner, D. Bhaskaran, R. Lennon, G. Grioli, M. Santello *et al.*, "The softhand pro: Functional evaluation of a novel, flexible, and robust myoelectric prosthesis," *PloS one*, vol. 13, no. 10, p. e0205653, 2018.

[8] J. Brooke *et al.*, "Sus-a quick and dirty usability scale," *Usability evaluation in industry*, vol. 189, no. 194, pp. 4–7, 1996.

A Novel Platform to Assess the Effects of the Rubber Hand Illusion on the Tactile Reference Frame

François Le Jeune, Marco D'Alonzo, Luigi Raiano, Domenico Formica and Giovanni Di Pino

***Abstract*—The Rubber Hand Illusion (RHI) can be used to induce the illusion that a fake hand is part of one's own body. Thus, it can be used to alter the body representation. It was also reported that the RHI induces a proprioceptive drift (PD) of one's real hand toward the fake hand. The RHI can be induced when the fake hand is placed farther in the sagittal plane (distally) compared to the real hand. In this case, the induced update of the body representation is an elongation of the arm. In a previous study, performing the Tactile Distance Perception Task (TDPT) with the proximo-distal RHI, it has been shown that the tactile distance increases after the proximo-distal RHI. However, the setup presented some limits: the rubber hand was medially misaligned compared to the real hand and the elongation range was too small.**

To tackle these issues, we developed a novel platform consisting in a virtual reality (VR) application integrating an optical motion capture device and haptic stimulators that enables to perform the RHI without any misalignment and with a wide range of elongation.

I. Introduction

THE sense of body ownership refers to the particular perceptual status when part of one's own body is identified as self. The Rubber Hand Illusion (RHI) is a method employed to study the sense of body ownership. It is performed by congruently brush-stroking a visible fake hand and the hidden real hand of a participant, while the participant is observing the fake hand. It is used to induce the illusion that a fake hand is part of a participant's own body. Thus, the illusion that arises can be used to alter the body representation. It has been reported that the RHI also induces a subjective drift of the participant's real hand towards the fake hand, called the proprioceptive drift (PD) [1]. Usually, the fake hand is placed closer along the frontal plane with respect to the real hand (medially), and the illusion induces a latero-medial drift of the perceived real hand's position. However, it has been shown that the RHI can also be induced when the fake hand is placed farther along the sagittal plane with respect to the real hand (distally). In this case, the induced update of the body representation is an elongation of the arm, and the PD is directed proximo-distally.

The tactile distance perception task consists in assessing the sense of distance between two simultaneous tactile contacts on a subject's body part. It can be performed before and after inducing the proprioceptive illusion that the concerned body part is elongated or shrunk.

Would the update of the body representation induced by a distal RHI, i.e. an elongation of the arm, affect the tactile reference frame, thus the tactile distance between two points? To assess this hypothesis, we formerly tested a protocol in real environment. Howerver, it proved to be limited by two factors. First, the rubber hand was misaligned in the sagittal plane compared to the real hand. Secondly, the elongation range was too small. To tackle these issues, we developed a novel platform consisting in a virtual reality (VR) application integrating an optical motion capture device and haptic stimulators that enable to perform the RHI without any misalignment and with a wide range of elongation.

II. Material and Methods

A. Real environment

In the real environment, the subject is seated comfortably in a chair in front of a table and is equipped with the VR head mounted device (HMD) covering the eyes. They are positioned at the center of the motion capture workspace while VR infrared cameras are placed outside of the workspace, oriented towards the HMD.

B. VR application

The VR application is developed with Unity 2018.3.0f2 (Unity Technologies). The VR hardware equipment used is the HTC Vive kit consisting in the HMD and two infrared cameras. In the virtual environment, participants see their virtual body coincident with their real body in a first-person perspective. The participants' avatar is seated in front of a table and the virtual experimenter faces it, seated on the other side of the table, in a room similar to the real one. The experimenter is holding a virtual paint brush in the right hand to perform the stroking on the participant's left hand. When animated, the experimenter avatar performs the brush-stroking of the subject's avatar's left hand's index. The brushing movement is reproduced from a previous motion capture recording of a real experimenter performing the brush-stroke. The proximo-distal displacement of the fake hand can be reproduced in the VR environment by elongating the forearm of the subject's avatar by 20 or 40 cm.

François Le Jeune, Marco D'Alonzo, Luigi Raiano, Domenico Formica, and Giovanni Di Pino are with NeXT Lab, Università Campus Bio-Medico di Roma. (f.lejeune@unicampus.it)

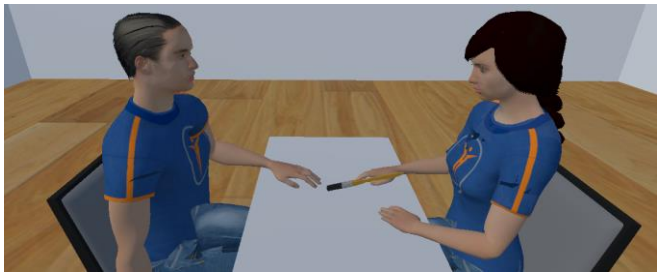

Fig. 1. Visualization of the VR application environment.

C. *Motion Capture*

To track the movement of the subject, an Optitrack motion capture system (Natural Point, Inc.) has been used. The motion capture hardware consists in 4 Prime 13W optical cameras placed on the top corners of a cubic metallic structure. Optical markers are attached to the participant's left arm and left forearm to track their movements and reproduce them accordingly on the virtual avatar. This is done to maximize the subject's embodiment of the virtual body. The markers positions are processed through Optitrack's Motive software (version 2.1.1 Final), and live streamed to the VR application in Unity.

The left hand and its fingers movements are also tracked, but using a Leap Motion device (Leap Motion, Inc.) mounted on the HTC Vive HMD. Their movements are also live streamed to the VR application and reproduced on the subject avatar's left hand and its fingers.

D. *Haptic stimulation*

The haptic stimulation is performed thanks to a small 3D printed robotic arm holding a paintbrush. The robotic arm has one degree of freedom and is actuated by a brushed DC motor (Pololu Corporation, USA). It is designed in order to reproduce the typical brushing pattern of a human experimenter. The motor is controlled by prototyping board (STMicroelectronics, Switzerland) and an Olimex controller (Olimex, Bulgaria). The brush of the robot is equipped with a piezo-electric sensor that detects the contact between the brush and the index finger of the subject in order to synchronize the movement of the robot with the movement of the virtual brushing. The haptic stimulation can be performed congruently or incongruently with respect to the visual virtual brushing.

III. Experimental Procedure

The first part of the experimental protocol consists in a familiarization phase of the subjects with the virtual avatar in order to make them prone to its embodiment. In the virtual environment the subject's avatar is seated on a chair in front of a table and the experimenter is seated on the other side, arms crossed. The motion tracking of the arm, hand and fingers of the subject is activated, and the subjects can move their left arm and hand freely while they see their avatar moving accordingly. The right arm of the subject remains still and along the body during the whole experiment.

When the subject is ready, the experimental phase can start. In this phase, the subject arm and hand are still, and the hand is placed at rest, palm down on the table.

Six conditions per subjects will be tested. A synchronous and an asynchronous brushing (between the visual brushing and the haptic stimulation) will be performed for each elongation size or the arm: 0 cm, 20 cm, and 40 cm. The conditions will be tested in a random order for every subject.

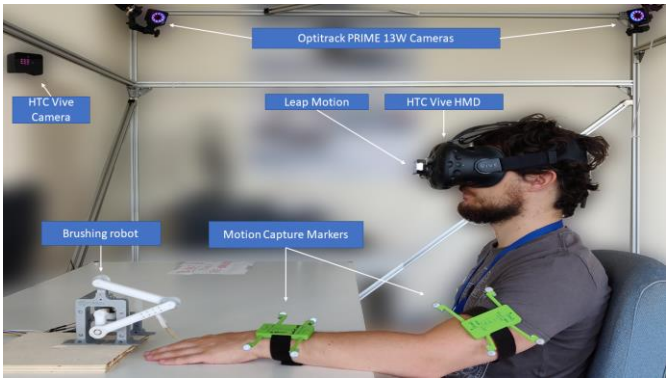

Fig. 2. Hardware setup of the platform.

IV. Conclusion and Future Work

We developed a novel platform to assess the effects of a proximo-distal version of the RHI on the tactile reference frame of the left arm. It can now be used to perform the experiment it is meant to.

A future work is to improve the tracking of the hand by using the Optitrack system. To do so, we would have to refine the tracking of the fingers and to develop our own functionality to live stream the skeleton of the hand from Motive to Unity.

Furthermore, a panel of esthetic features could be added to the subject's avatar to fit the subject's physical aspect and improve the feeling of embodiment.

Finally, this platform could be used for two possible future applications. One could be to help understand the process behind the formation of the internal image of the body. The other one could be a possible therapeutic application for people with an altered image representation of their body caused by amputation or another upper limb trauma.

Acknowledgment

This work is part of the ERC Grant Projet RESHAPE: REstauring the Self with embodiable HAnd ProsthesEs.

References

[1] Botvinick M., Cohen J., Rubber hands "feel" touch that eyes see, Nature, 1998.

The effect of filtering and normalization on EMG feedback for prosthesis control

Jack Tchimino, Jakob Lund Dideriksen, Strahinja Dosen

***Abstract*—Closing the control loop in prosthetics is an important goal to improve the control and promote embodiment. Recently, a novel approach to provide feedback was presented, wherein the tactile stimulation is used to transmit the magnitude of the myoelectric signal to the prosthesis user. In the present study, we investigate how the processing of the EMG signal affects the performance of EMG biofeedback for prosthesis control. We focus on the effect that the low-pass filter cutoff frequency following a rectifier, used to provide the EMG envelope, and the percentage of the MVC to which the filter's output is normalized have on the control of grasping force of a prosthetic hand. These parameters have a direct effect on the sensitivity of the system and our goal is to narrow down the values that optimize said sensitivity and facilitate the control of the grasping force.**

I. Introduction

Loss of an upper limb is a traumatic event that severely impacts an amputee's daily life, by hampering their ability to perform everyday tasks. Prosthetic hands attempt to restore part of the lost functionality, with varying degrees of success. Arguably, the most popular method for control is the exploitation of surface electromyographic signals, as EMG-based prosthetics control systems currently dominate the market.

A very simple control scheme is that of proportional control, wherein the speed of the motors controlling the fingers in the prosthetic hand and, by extension, the force applied by it, are proportional to the amplitude of the EMG [1]. It is, however, difficult to achieve consistent and robust control of the grasp force by solely implementing a feedforward scheme. Feedback is essential for controlling and correcting the movement of the prosthesis, with electro- and vibrotactile feedback being the most prominent in literature [2].

A usual approach is to provide feedback on the prosthesis state (e.g. grasping force or joint angles). Recently, a different approach to feedback has been proposed [3], wherein the tactile stimulation transmits, instead, the prosthesis control input, in this case the EMG, thus allowing the subject to explicitly control the strength of their muscle contraction and, by extension, the force applied by the prosthesis, since it is proportional to the EMG. It was demonstrated that EMG feedback is more effective than classic force feedback when provided using a visual and electrotactile feedback interface. However, the effect of filtering and calibration of the EMG on the effectiveness of this novel feedback approach has not been investigated.

A common processing scheme for the EMG is the calculation of its linear envelope, [4], [5]. After filtering, the EMG is normalized to a percentage of the maximum voluntary contraction value (MVC) [3]. The closed-loop prosthesis control scheme is likely to be affected by the cutoff frequency and the MVC percentage to which the EMG is normalized. As the low-pass cutoff frequency decreases, the rapid changes in the EMG amplitude will be attenuate, therefore, it will be easier for the subject to modulate their muscle contraction using EMG feedback, at the expense of system response time, while a higher cutoff will produce a more noisy output and a more sensitive system. Similarly, normalizing to a lower MVC percentage will create larger responses at lower contractions, make the system more sensitive and the control more difficult; however, since the EMG is inherently less variable in smaller intensities, it can be argued that modulating in these intensities will actually facilitate control.

It is our hypothesis that there is a set of optimal values for the low-pass cutoff and the percentage of the MVC calibration that facilitate the control of the prosthesis. To that end, we have performed a parametric analysis, varying the values of these two parameters and investigating their effect on the proportional force control of a sensorless prosthetic hand. In the present study, the feedback was implemented using vibrotactile stimulation [3].

II. Material and Methods

A. Setup

The prosthesis used in the setup was a Touch Bionics RoboLimb, fixed in place using a custom-made base. A Vernier Hand Dynamometer is used to measure the force applied by the hand and its output voltage is routed into a NI USB-6212 acquisition board, digitized at 20 Hz. Four C2 vibration

This project was funded by the Danish Independent Research Fund.

Jack Tchimino, Jakob Lund Dideriksen and Strahinja Dosen are with the Sensory Motor Interaction Lab of the Health Science and Technology Department of Aalborg University, Aalborg, Denmark

tactors were placed on the subject's upper arm at a position that did not hinder elbow movement and were connected to a tactor control unit, both by Engineering Acoustics Inc. The subjects' wrist was immobilized using a thermoplastic splint. The EMG signals were recorded from the proximal part of the forearm using a wireless Thalmic Labs MyoBand device and were full-wave rectified and filtered using a second order low-pass Butterworth filter, whose output was normalized to a percentage of the MVC.

The EMG was quantized in four contraction zones of equal width, which also include a dead zone to eliminate responses to very low contractions (see Fig. 2). Each of the four contraction zones corresponds to a single vibration feedback spatial pattern, following the scheme in Fig.1., providing the subjects with information on the level of their myoelectric signal. The EMG was also transmitted to the prosthesis, to control its closing velocity and, by extension, the grasping force it applied.

B. Experimental Procedure

After a detailed explanation of the procedure and the goal of the experiment, the subjects were seated comfortably in front of a computer screen. The subjects were asked to flex their wrist against the splint (thus creating isometric muscle contractions) to the maximum level they would be able to maintain without fatiguing for 5 seconds. This was repeated three times, each time isolating the largest value recorded in all channels and then selecting the largest value over all the trials, which was used as the flexor muscles MVC. In addition, the channel with the largest amplitude was selected as the representative channel for the flexors and its signal used for control of the prosthesis and the feedback.

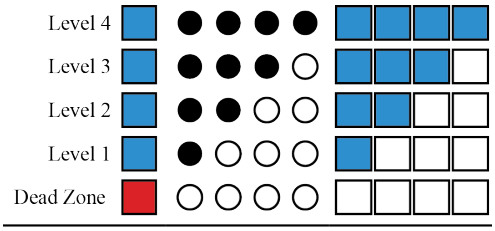

Fig. 1. The control and feedback scheme

A training period followed, in which the subjects were asked to freely open and close the prosthesis, while receiving feedback from the tactors and viewing the force level produced on the screen, so that the subjects can associate feedback patterns to contraction levels.

The main part of the experiment involves the generation of a random sequence of 40 target force levels, displayed in sequence on the screen, which the subjects must achieve by modulating their muscle contraction while receiving vibrotactile feedback. The subjects would then maintain this level, while the prosthesis closed around the dynamometer. If the subjects reached the proper EMG level, the prosthesis would produce the target force (the principle of EMG feedback).

A different set of parameters is used in every run of the experiment.

III. Results and Discussion

Part of the full protocol was tested in the preliminary pilot test, wherein four parameter sets were tested over a small number of repetitions. Here, we present only the myoelectric signals generated by a single subject, to highlight EMG modulation. These results can be extrapolated to grasp force production, since different levels of EMG can be mapped to different finger velocities and, thus different force levels.

The results in Fig. 3. showed that a difference in the MVC calibration had no significant effect on the ability of the subjects to modulate their EMG using online feedback. However, a higher cutoff frequency caused the output to be more irregular and jump across different levels, thus reducing the robustness of the prosthesis control scheme. In this case, it was substantially more difficult for the subject to maintain a steady contraction to generate the desired level of EMG using the online feedback.

A full run of experiments has been scheduled, leading to a more complete investigation, which will provide a clearer picture of how these two parameters affect EMG control.

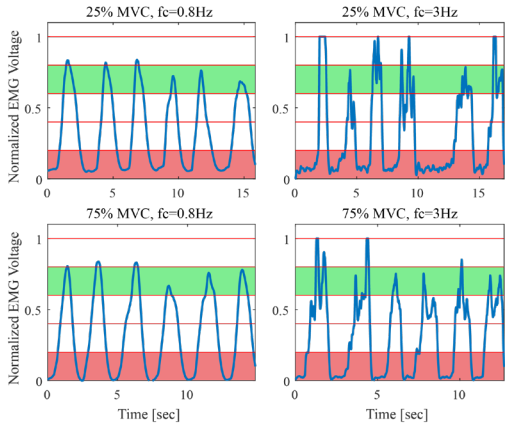

Fig. 2. The normalized EMG for four different parameter sets. The dead zone is highlighted with red, while the target contraction level is highlighted in green.

IV. References

[1] A. Sturma *et al.*, "A surface EMG test tool to measure proportional prosthetic control," *Biomed. Eng. / Biomed. Tech.*, vol. 60, no. 3, pp. 207–213, Jan. 2015.

[2] P. Svensson, U. Wijk, A. Björkman, and C. Antfolk, "A review of invasive and non-invasive sensory feedback in upper limb prostheses," *Expert Rev. Med. Devices*, vol. 14, no. 6, pp. 439–447, 2017.

[3] S. Dosen, M. Markovic, K. Somer, B. Graimann, and D. Farina, "EMG Biofeedback for online predictive control of grasping force in a myoelectric prosthesis," *J. Neuroeng. Rehabil.*, vol. 12, no. 1, pp. 1–13, 2015.

[4] M. A. Schweisfurth, M. Markovic, S. Dosen, F. Teich, B. Graimann, and D. Farina, "Electrotactile EMG feedback improves the control of prosthesis grasping force," *J. Neural Eng.*, vol. 13, no. 5, p. 056010, Oct. 2016.

[5] O. Barzilay and A. Wolf, "A fast implementation for EMG signal linear envelope computation," *J. Electromyogr. Kinesiol.*, vol. 21, no. 4, pp. 678–682, Aug. 2011.

Mutual comparison of different neural networks in identification of motor unit firings from high-density surface electromyograms

F. Urh, A. Holobar, D. Strnad

***Abstract*— Despite all the research efforts in the last few years, accurate identification of motor unit (MU) firings from high-density surface electromyograms (HDsEMG) still presents a major scientific challenge. Different decomposition methods have been proposed, each with its advantages and limitations. In this study, we investigated the capability of deep neural networks (NN) to directly estimate motor unit firings from HDsEMG signals. Different types of NN and their structures were tested and mutually compared. We discuss their limitations and efficiency in identification of individual motor units, along with the speed and stability of their training. Evaluation was done on signals with different noise levels. We observed that LSTM and convolutional NN yield significantly more true positive (TP) and less false positive (FP) and false negative (FN) MU spikes than dense NN.**

I. Introduction

In recent years, neural networks (NN) experienced a huge breakthrough in development, mostly because of constantly increasing computer processing power. Dedicated hardware has also been developed to process NN even faster [8]. Consequently, more complex NN models have been developed, with a large number of layers. It was shown that these NN really improve the state of the art, especially in the fields of image processing, speech recognition, and natural language processing [6], [7].

On the other hand, accurate identification of motor unit (MU) firings from high-density surface electromyograms (HDsEMG) is still not a fully resolved problem. Today's most used methods for identification of MU firings are based on mathematical HDsEMG models and advanced signal processing techniques [2], [9]. In this study, we evaluated performance of different NN to predict MU firings directly from HDsEMG signals.

II. Neural networks evaluation

For NN evaluation, we used synthetically generated motor unit action potentials (MUAPs) as described in [3] and convolved them with predetermined MU firing patterns, generated by the model in [1]. The simulated signals were 10 seconds long and sampled at 2048 Hz. We simulated 200 MUs at constant excitation level of 30 %, which resulted in 155 active MUs. We added noise with SNR = ∞, 30 and 20 dB. Afterwards, Convolution Kernel Compensation (CKC) decomposition method [2] was used to identify MU firings. From all the obtained MUs we discarded those with Pulse-to-Noise Ratio (PNR) [3] below 28 dB, keeping 49, 9 and 5 MUs for SNR = ∞, 30 and 20 dB. HDsEMG signals were extended with a factor 10 and spatially whitened [2]. The signals were then split into train, validation and test datasets, with the length of 5, 2.5 and 2.5 seconds, respectively. On average, there were 62.9 ± 21.3, 39.7 ± 24.0 and 24.0 ± 3.5 MU firings in the test set at SNR = ∞, 30 and 20 dB, respectively.

The following three different types of NN, detailed in Table I, were used to predict MU firings from HDsEMG signals:

a) Dense NN – a feedforward NN, where all the neurons in a layer are connected to those in the next layer.

b) LSTM NN [5] – a recurrent NN with feedback connections, where some of neurons' outputs from a layer are connected to neurons in the previous layer.

c) Convolutional NN – a feedforward NN that uses convolution in at least one of the layers.

TABLE I: Layers of NN used in this study named as in the machine learning package TensorFlow.

Dense NN	LSTM NN	Convolutional NN
dense [450] *	lstm [15, 100] *	conv2d [36, 6, 128]
dense [250] *	lstm [75] *	max_pooling2d [18, 3, 128] *
dense [100] *	dense [50] *	conv2d [8, 2, 128]
dense [50] *	dense [25] *	max_pooling2d [4, 1, 128] *
dense [1]	dense [1]	flatten [512]
		dense [128] *
		dense [32] *
		dense [1]

Values in [] denote output size of the layer without batch size. * indicates a layer to which a dropout layer with a rate of 0.2 was applied.

Each NN received HDsEMG signals as the input and predicted firings of selected MU on the output. Multiple MUs with different characteristics (firing frequency, PNR) were used for evaluation. The generated HDsEMG signals had 90 channels and because of extension by factor 10, we got a vector of 900 values per each HDsEMG sample. In the case of dense NN, we put one such vector at the NN input per iteration. In the case of LSTM and convolutional NN, 15 vectors were joined together into a 900×15 matrix. NN were trained by Adam optimizer [4], with initial learning rate set to 0.001. Mean squared error was used as a loss function and hyperbolic tangent as activation function. Training was done for 500 epochs but could have finished before, if loss metric on validation dataset didn't improve after 20 iterations. The batch size was set to 128 samples.

This study was supported by the Slovenian Research Agency (projects J2-7357, J2-1731 and L7-9421 and Programme funding P2-0041).

F. Urh, A. Holobar and D. Strnad are with the Faculty of Electrical Engineering and Computer Science, University of Maribor, Maribor, Slovenia (corresponding author: filip.urh1@um.si).

III. Results

The results of NN-based MU identification are presented in Figs. 1 and 2. For statistical analysis we used non-parametric Friedman test with Bonferroni correction and p-value < 0.05, because in 63 % of MUs the normal distribution of true positives (TPs), false positives (FPs) and false negatives (FNs) was rejected by Lilliefors test.

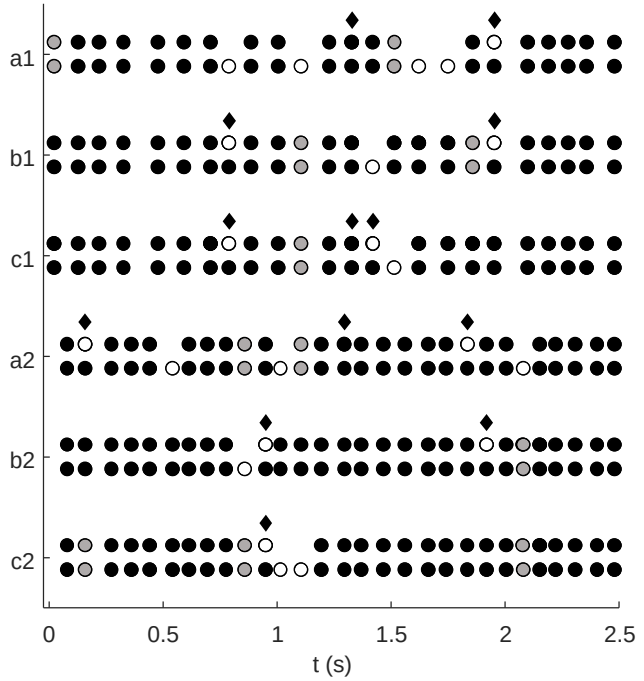

Fig. 1. Prediction visualization of two MUs (1, 2) with dense (a), LSTM (b) and convolutional NN (c). Each result is composed of two rows, where the bottom row depicts the true values, and the top row the predicted ones. Filled circles represent a match between reference and predicted values, empty circles no match and gray circles a match with tolerance of 5 samples. The diamond depicts two consequently predicted pulses within a range of 5 samples.

IV. Discussion

LSTM and convolutional NN converged faster than dense NN. On average, the number of training epochs was 263 ± 52, 142 ± 37 and 187 ± 46 for dense, LSTM and convolutional NN, respectively. Fig. 2 demonstrates that LSTM and convolutional NN also yield significantly more TP and less FP and FN pulses than dense NN. These two NN also have relatively small absolute number of FPs, though the number of FNs is not negligible. These conclusions apply to all the tested SNR levels. However, the number of TPs vs. number of FNs ratio is higher with higher SNR value.

One of the possible reasons why this relatively simple NN models didn't detect more firings, may be the fact that learning size (number of samples) during the NN training was relatively small. It is widely known that with smaller learning datasets ease of NN fitting improves, whereas generalization deteriorates.

The one obvious drawback with this kind of NN learning is the need for a few already identified MU firings, so that NN can learn how to predict them. There is a possibility to avoid this, but different types of NN with support for unsupervised learning must be used for this purpose.

In conclusion, the NN-based prediction of motor unit firings directly from HDsEMG signals is a promising technique that can be used alongside today's decomposition methods. However, further studies are required to find optimal NN structure and training parameters. Additionally, evaluation and performance on experimental signals, recorded in different conditions, must be assessed.

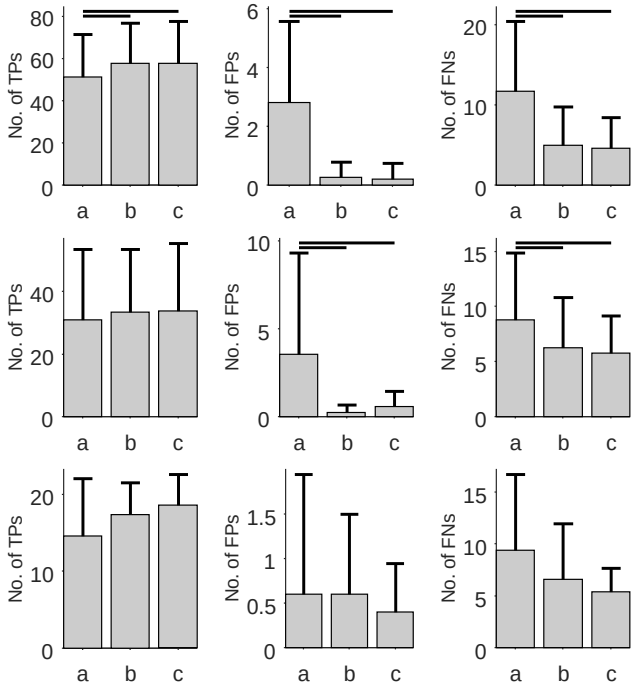

Fig. 2. Number of TPs, FPs and FNs (mean + SD) for dense (a), LSTM (b) and convolutional (c) NN at SNR values of ∞ (top row), 30 dB (central row) and 20 dB (bottom row). Horizontal line above bars depict statistically significant difference confirmed by Friedman test (p-value < 0.05).

References

[1] A. J. Fuglevand, D. A.Winter, and A. E.Patla, "Models of recruitment and rate coding organization in motor-unit pools," *J. Neurophysiol.*, vol. 70, no. 6, pp. 2470–2488, Dec. 1993.

[2] A. Holobar and D. Zazula, "Multichannel Blind Source Separation Using Convolution Kernel Compensation," *IEEE Trans. Signal Process.*, vol. 55, no. 9, pp. 4487–4496, Sep. 2007.

[3] A. Holobar, M. A. Minetto, A. Botter, F. Negro, and D. Farina, "Experimental analysis of accuracy in the identification of motor unit spike trains from high-density surface EMG," *IEEE Trans. Neural Syst. Rehabil. Eng.*, vol. 18, no. 3, pp. 221–229, Jun. 2010.

[4] D. P. Kingma and J. Ba, "Adam: A Method for Stochastic Optimization," *arXiv preprint*, arXiv:1412.6980, 2014.

[5] S. Hochreiter and J. Schmidhuber, "Long Short-Term Memory," *Neural Computation*, vol. 9, no. 8, pp. 1735-1780, Nov. 1997.

[6] Y. LeCun, Y. Bengio, and G. E. Hinton, "Deep learning," *Nature*, vol. 521, pp. 436-444, May 2015.

[7] A. Krizhevsky, I. Sutskever, and G. E. Hinton, "ImageNet Classification with Deep Convolutional Neural Networks," *Advances in Neural Information Processing Systems*, pp. 1097-1105, May 2012.

[8] N. P. Jouppi, et al. "In-datacenter performance analysis of a tensor processing unit.", *ACM/IEEE 44th Annual International Symposium on Computer Architecture*, 2017.

[9] M. Chen and P. Zhou, "A Novel Framework Based on FastICA for High Density Surface EMG Decomposition," *IEEE Trans. Neural Syst. Rehabil. Eng.*, vol. 24, no. 1, pp. 117–127, Jan. 2016.

Finger force perception during pressing tasks: Comparison of force matching and psychophysical reports.

Cristian J. Cuadra and Mark L. Latash

***Abstract*— We used force-matching tasks between the two hands and verbal report to test predictions of the scheme of perception based on the concept of iso-perceptual manifold (IPM). Our hypothesis was that accuracy and variability of individual finger force matching would be worse in a two-finger task compared to one-finger tasks. The subjects produced accurate forces under visual feedback by pressing with either all two fingers or by one of the fingers of the task-hand. They tried to match the total two-finger force or individual finger forces by pressing with the other hand (match-hand, no visual feedback) adding the verbal report of force perception. The match-hand consistently overshot the task-hand force. Verbal report always underestimated the force that the task-hand was producing. These findings confirm our main hypothesis by showing that perception of individual finger forces vary in multi-finger tasks within a space (IPM) corresponding to veridical perception of total force.**

I. Introduction

We explored a recently introduced scheme of perception based on the concept of iso-perceptual manifold (IPM) in the combined afferent–efferent space of neural signals [1]. Within this scheme, we assume that afferent (sensory) signals from multiple sources are estimated within a frame of reference provided by the multiple ongoing efferent processes that can be adequately described as time-varying spatial reference coordinates [1] - [5]. An IPM is equivalent to stable perception of a physical variable. We used force-matching tasks between the two hands, and verbal reports, to explore finger force perception in a two-finger pressing task. The main hypothesis was that accuracy would be lower and variability higher during individual finger force matching in a two-finger task compared to one-finger tasks.

II. Material and Methods

A. Methods

9 subjects (5 males and 4 females, ages between 25 to 32 years, mass 73±10 kg, height 1.67±0.5 m) volunteered in the study. All subjects self-identified as right-handed according to the preferred hand used during writing and eating. The subjects were healthy, had no history of hand injury or neuromotor disorder, and provided written informed consent in accordance with procedures approved by the Office for Research Protections at The Pennsylvania State University.

B. Procedure

Subjects were asked to produced accurate force levels under visual feedback by pressing on force sensors with either two fingers or one of the fingers of a hand (task-hand). They tried to match the total two-finger force or individual finger forces by pressing with the other hand (match-hand, no visual feedback). Also, we used verbal report within a psychophysical scale on the level of force that the task-hand was producing.

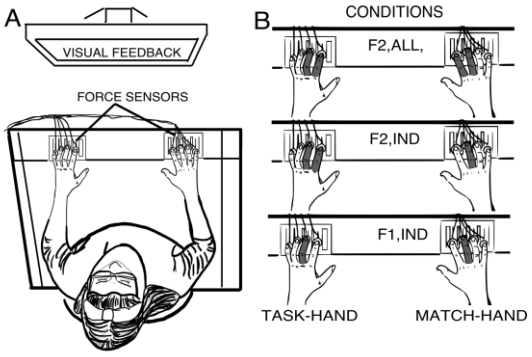

Fig. 1. A: An illustration of the top view of the setup showing the position of the subject, the location of the force sensors, and the monitor used for visual feedback. B: Conditions used during the experiment, where the left hand represents the task-hand and the right hand represent the match-hand. The shaded finger(s) represent the finger(s) that was (were) required to produce force within each hand for the three conditions of the experiment ($F2_{ALL}$, $F2_{IND}$, and $F1_{IND}$). F2 and F1 refer to two-finger and single-finger force production by the task-hand, respectively. ALL refers the condition when all the fingers of the match-hand try to match the total force of the task-hand. "IND" refers to the condition when the matching process is produced by one of the fingers (IND= I – index and M – middle) while the task-hand was performing wither two-finger or one-finger task ($F2_{IND}$ and $F1_{IND}$ conditions, respectively).

C. Apparatus

Four Nano-17 six-axis force/torque transducers (ATI Industrial Automation, Apex, NC) were used to record the

The study was in part supported by an NIH grant R21 NS095873, UPAC fund and UNAB-Chile travel grant.

Finger force perception during pressing tasks: Comparison of force matching and psychophysical reports.

C. C. Author is with Department of Kinesiology, The Pennsylvania State University, University Park, PA 16802, USA, and Escuela Kinesiología, Facultad de Ciencias de la Rehabilitación, Universidad Andres Bello, Calle Quillota 980, Viña del Mar, Chile (corresponding author to provide e-mail: cjc41@psu.edu).

M. L. Author, is with Department of Kinesiology, The Pennsylvania State University, University Park, PA 16802, USA.

normal forces from the index (I) and middle (M) fingers of both hands.

Finger force signals were amplified using the factory-calibrated interface (ATI Industrial Automation). Data were sampled at 1000 Hz with two PCI-6225, 16-bit, analog-to-digital cards (National Instruments, Austin, TX). A customized LabVIEW-based software was developed to log data for offline analysis and provide visual feedback to the experimenter and to the subjects (as needed) via a 20" monitor placed 1 m away at eye level. The experimental setup is shown in Figure 1.

III. Results

The match-hand showed higher inter-trial force variability during single-finger matching when the task-hand performed the two-finger task compared to trials when the task-hand performed single-finger tasks (Fig. 3). The match-hand overestimated the force of the task-hand at low forces and underestimated it at high force (Fig. 2A). The verbal report consistently underestimated the task-hand force, with larger errors for higher forces (Fig. 2B). These findings confirm our main hypothesis by showing that perception of individual finger forces can vary in multi-finger tasks within a space (IPM) corresponding to veridical perception of total force. Matching hypothetical commands to fingers, rather than finger forces, could be responsible for the force overshoots.

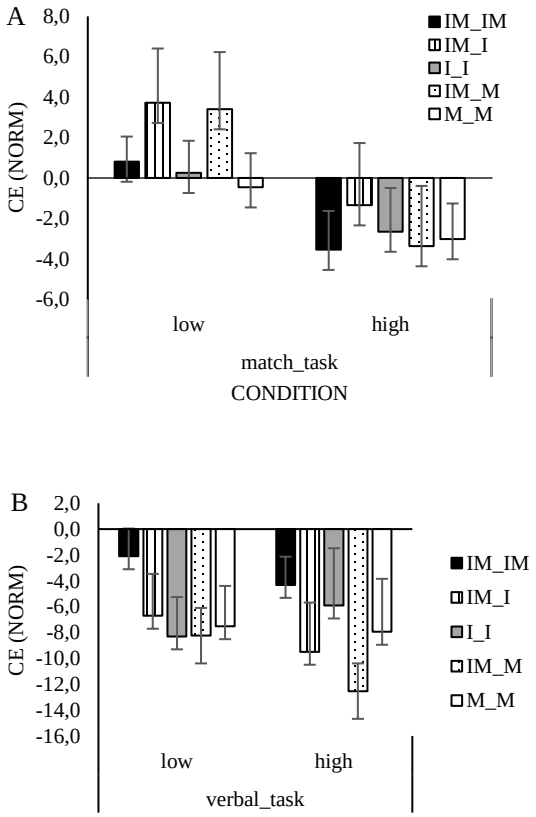

Fig. 2. Constant error (CE) values averaged across subjects with standard error bars for the two-finger (F2) condition and single-finger (F1) condition, for forces values (panel A). At panel B, we find CE for verbal report versus task-hand force values averaged across subjects. Note that the subjects consistently overshot the task-hand force for low level of forces, and not for the high level. Verbal report always underestimates the level of force that the task-hand produced.

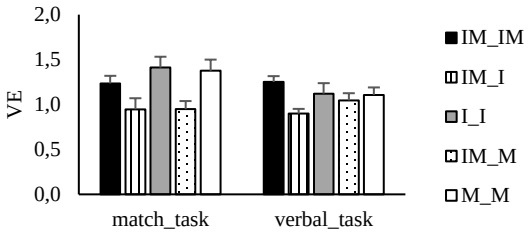

Fig. 3. VE measured as the R^2 (z-transformed) of force computed across trials for both match-hand vs task-hand and verbal report vs task-hand. The data are averages across subjects with standard error bars. Note the larger R^2 values for the match- task condition compared to verbal-task condition. Also, larger R^2 for the F1 condition compared to the F2 condition..

IV. Discussion

The main hypothesis has been supported in the experiment. Indeed, individual finger force matching in the two-finger task showed smaller R^2 compared to the one-finger tasks. This was predicted based on the idea that percepts of individual finger forces could vary across trials within the IPM for perception of the task-related total hand force, F_{TOT}.

V. Conclusion

The IPM concept suggests that perception accuracy for a given element may differ across tasks involving this element alone and involving a set of elements [2], [6]. In the latter case, percepts of elements are free to move over the corresponding IPM without violating perception of the salient variable produced by the set. Hence, one can expect larger inter-trial variability of elements in multi-element tasks compared to single-element tasks as shown in results of this experiment.

References

[1] M. L. Latash (2018) Stability of kinesthetic perception in efferent-afferent spaces: The concept of iso-perceptual manifold. Neurosci 372: 97-113.

[2] C. Cuadra, M. L. Latash (2019). Exploring the Concept of Iso-perceptual Manifold (IPM): A Study of Finger Force-Matching Tasks. Neuroscience, 401, 130–141. https://doi.org/10.1016/j.neuroscience.2019.01.016

[3] A.G. Feldman (2016) Active sensing without efference copy: referent control of perception. J Neurophysiol 116: 960-976.

[4] A.G. Feldman, M. L. Latash (1982) Interaction of afferent and efferent signals underlying joint position sense: Empirical and theoretical approaches. J Mot Behav 14: 174-193.

[5] S. Ambike, D. Mattos, V.M. Zatsiorsky, M. L. Latash (2016) Synergies in the space of control variables within the equilibrium-point hypothesis. Neurosci 315: 150-161.

[6] U. Proske, S. C. Gandevia (2012) The proprioceptive senses: their roles in signaling body shape, body position and movement, and muscle force. Physiol Rev 92, 1651-1697.

Study of the use of intramuscular sensors for electromyography detection and robotic systems for incomplete spinal cord injury

Camila R. Carvalho, Marvin Fernández, Filipe O. Barroso, Juan C. Moreno and José L. Pons

Abstract— **Spinal cord injury (SCI) affects more than 250 thousand people worldwide every year. The use of robots in SCI rehabilitation brings benefits for both the patient and the therapist, namely by proving more, accuracy, and variety of training modes, providing new outcomes to rehabilitation. Electromyography (EMG) activity onset is often used to trigger orthosis, prosthesis and exoskeletons in robotic rehabilitation. EMG can be recorded using either surface or intramuscular detection systems. The use of intramuscular electrodes, when compared with superficial ones, allows the detection of electric potentials closer to the muscle fibres and the registration of EMG activity from deeper muscles. European project EXTEND, where this paper is inset has, as of purpose, to develop neural interfaced assistive wearable robots for spinal cord injury. In this context, it was performed the analysis of the viability on the use of intramuscular EMG recordings to future application in the control of an exoskeleton.**

I. INTRODUCTION

SPINAL Cord Injury (SCI) can be defined as the total or partial loss of sensory and motor pathways and could reduce functional capacity, as the result of muscle recruitment and motor planning [1].

Recent advances in mechatronics design and embedded systems have led to the proliferation of wearable assistive devices that can provide locomotion assistance by actuating lower-limb joints. Such devices include robotic lower-limb prostheses, orthoses, and exoskeletons [2]–[6].

Assistive devices should support self-initiated movements for intuitive interaction and assist the SCI patients as naturally as possible [7], [8]. The muscular activity gives a representation of what the user is attempting to do and can be used to proportionally determine the torque generated by actuators in the device [6]. For that reason, electromyographic (EMG) activity is often used to control orthosis, prosthesis and exoskeletons in robotic rehabilitation [9]–[12].

EMG can be recorded using either surface or intramuscular electrodes. The use of intramuscular electrodes allows the detection of electric potentials closer to the muscle fibres besides allowing the registration of EMG activity from deeper muscles [13].

In this context, the European project EXTEND was created to develop a new concept of Bidirectional Hyper-Connected Neural Systems (BHNS) to extend the capabilities of neural interfaces with minimally invasive communication links between many nerves in the body and multiple external devices.

This paper is embedded in the EXTEND project and will comparatively evaluate lower limb intramuscular versus surface EMG signals in healthy subjects to analyze the viability of the use of intramuscular recordings to future application in the control of an exoskeleton for incomplete spinal cord injury.

II. MATERIALS AND METHODS

The experiments were performed in the National Hospital for Paraplegics of Toledo (SESCAM). Nine (9) healthy patients with ages between 20 and 40 years old participated in the experiments. The experimental protocol was divided into two phases:

- **Phase 1: muscle contraction assisted by an exoskeleton.** Subjects performed ten extension/flexion movements of the knee and ankle consecutively. In this phase, the data were obtained to understand the possible degradation of intramuscular signal due to electrode displacements during the movement assisted by the robotic exoskeleton.
- **Phase 2: muscle contraction without the exoskeleton.** The same tasks performed in Phase 1 were repeated, with the exoskeleton on. The information obtained in this phase was used to compare the performance of intramuscular and surface EMG recordings without the disturbances caused by the exoskeleton.

Quattrocento amplifier from OT Bioelettronica was used. Intramuscular EMG was recorded with wire electrodes from Spes Medica, and surface recordings were performed with Ambu electrodes. The exoskeleton used in the experiments is the Exo-H2 developed by the company Technaid S.L. Surface and intramuscular were acquired from the following muscles: Tibialis Anterior (TA), Gastrocnemius Medialis (GM), Biceps Femoris (BF) and Vastus Lateralis (VL).

III. RESULTS

General results showed the surface recordings presented muscle activation in a more significant number of channels when compared with the intramuscular. This result can be due to the displacement from the wire of the intramuscular

This project was funded by the European Union's Horizon 2020 research and innovation programme (Project EXTEND - Bidirectional Hyper-Connected Neural System) under grant agreement No 779982.

C. R. Carvalho is with the Neural Rehabilitation Group of the Spanish National Research Council, Madrid, Spain (corresponding author: camila.rodrigues@cajal.csic.es).

M. Fernández, is with CEU San Pablo University and with the Neural Rehabilitation Group of the Spanish National Research Council, Madrid, Spain.

F. O. Barroso is with the Neural Rehabilitation Group of the Spanish National Research Council, Madrid, Spain.

J. C. Moreno is with the Neural Rehabilitation Group of the Spanish National Research Council, Madrid, Spain.

J. L. Pons is with the Northwestern University and the Legs & Walking AbilityLab, Shirley Ryan AbilityLab, Chicago.

Fig. 1. Setup of the experimental protocol. In the left, subject with the exoskeleton and, in the right, the positioning of both EMG eletrodes acquisition system.

electrode, that leads to several losses of signal. However, when looking to the tasks with the exoskeleton, intramuscular recordings presented less affectation by the external robotic system. Figure 2 shows, in the left, taskx performances without the exoskeleton and in the right, with the exoskeleton.

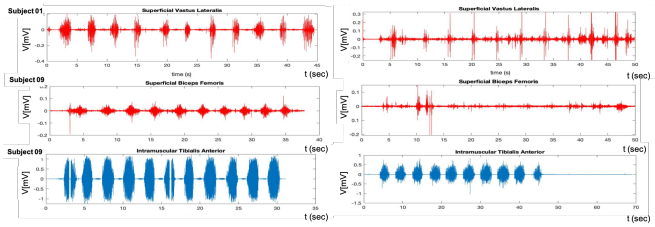

Fig. 2. Results of intramuscular and surface electrodes without (left) and with (right) the exoskeleton. In blue the intramuscular signals and in red the surface ones.

The SNR ratio was calculated to have a numerical tool to allow the comparison of the recordings obtained. The RMS average values of all subjects were calculated, as shown in 1.

$$SNR_{dB} = 10log_{10}\left(\frac{RMSsignal}{RMS_{noise}}\right)^2 \quad (1)$$

The result is shown in Figure 3. Surface recordings presented a higher SNR value, that can be explained by its amplitude, usually higher than the intramuscular recordings.

Average SNR									
Muscle	Knee Mov.		Knee Mov. Exo.		Muscle	Ankle Mov.		Ankle Mov. Exo.	
	Intra.	Sup.	Intra.	Sup.		Intra.	Sup.	Intra.	Sup.
VL	15,68	22,92	4,86	17,04	TA	77,64	37,56	12,34	23,83
BF	6,30	26,86	5,27	13,86	GM	6,54	14,26	1,76	12,07

Fig. 3. SNR average values for all nine subjects.

IV. Conclusion

Results have shown that, in general, there is more muscle activation detection with superficial recordings, what can be due to several reasons as, the facility of the electrode colocation and visual feedback. It is important to remark that, although intramuscular signals are not present in every muscle as expected, it could be possible to characterize the proposed tasks with a subset of solid electrodes and signals. The use of an exoskeleton, in this experiment's context, influenced the signal recordings, mostly in the surface signals, what can be due to the direct contact that the exoskeleton has with the electrodes once, it was also observed that the intramuscular recordings present less signal distortion than the superficial when using the exoskeleton. In general, the experiments showed positive results, but, further experimentation must be done to concrete the proposed goals.

V. Acknowledgment

This project was funded by the European Union's Horizon 2020 research and innovation programme (Project EXTEND - Bidirectional Hyper-Connected Neural System) under grant agreement No 779982.

References

[1] L. J. Holanda, P. M. M. Silva, T. C. Amorim, M. O. Lacerda, C. R. Simão, and E. Morya, "Robotic assisted gait as a tool for rehabilitation of individuals with spinal cord injury: a systematic review," *Journal of NeuroEngineering and Rehabilitation*, vol. 14, no. 1, p. 126, 2017.

[2] B. Hu, E. Rouse, and L. Hargrove, "Fusion of bilateral lower-limb neuromechanical signals improves prediction of locomotor activities," *Frontiers Robotics AI*, vol. 5, no. JUN, pp. 1–16, 2018.

[3] H. A. Varol, F. Sup, and M. Goldfarb, "Multiclass real-time intent recognition of a powered lower limb prosthesis," *IEEE Transactions on Biomedical Engineering*, vol. 57, no. 3, pp. 542–551, 2010.

[4] L. M. Mooney, E. J. Rouse, and H. M. Herr, "Autonomous exoskeleton reduces metabolic cost of walking," *2014 36th Annual International Conference of the IEEE Engineering in Medicine and Biology Society, EMBC 2014*, pp. 3065–3068, 2014.

[5] F. A. Panizzolo, I. Galiana, A. T. Asbeck, C. Siviy, K. Schmidt, K. G. Holt, and C. J. Walsh, "A biologically-inspired multi-joint soft exosuit that can reduce the energy cost of loaded walking," *Journal of NeuroEngineering and Rehabilitation*, vol. 13, no. 1, 2016.

[6] A. J. Young and D. P. Ferris, "State of the art and future directions for lower limb robotic exoskeletons," *IEEE Transactions on Neural Systems and Rehabilitation Engineering*, vol. 25, no. 2, pp. 171–182, 2017.

[7] D. Ruy Soprani S. Araujo, T. Rodrigues Botelho, C. Rodrigues C. Carvalho, A. Frizera, A. Ferreira, and E. Rocon, "Platform for Multimodal Signal Acquisition for the Control of Lower Limb Rehabilitation Devices," in *Proceedings of the 2nd International Congress on Neurotechnology, Electronics and Informatics (NEUROTECHNIX-2014)*, pp. 49–55, 2015.

[8] J. Ibáñez, J. Serrano, M. del Castillo, J. Gallego, and E. Rocon, "Online detector of movement intention based on EEG—Application in tremor patients," *Biomedical Signal Processing and Control*, vol. 8, pp. 822–829, nov 2013.

[9] E. A. Kirchner, M. Tabie, and A. Seeland, "Multimodal movement prediction - Towards an individual assistance of patients," *PLoS ONE*, vol. 9, no. 1, 2014.

[10] E. E. Cavallaro, J. Rosen, J. C. Perry, and S. Burns, "Real-time myoprocessors for a neural controlled powered exoskeleton arm," *IEEE Transactions on Biomedical Engineering*, vol. 53, no. 11, pp. 2387–2396, 2006.

[11] L. M. V. Benitez, N. Will, M. Tabie, S. Schmidt, E. Kirchner, and J. Albiez, "An EMG-based Assistive Orthosis for Upper Limb Rehabilitation," pp. 323–328, 2013.

[12] L. M. Vaca Benitez, M. Tabie, N. Will, S. Schmidt, M. Jordan, and E. A. Kirchner, "Exoskeleton technology in rehabilitation: Towards an EMG-based orthosis system for upper limb neuromotor rehabilitation," *Journal of Robotics*, vol. 2013, no. September 2015, 2013.

[13] R. Merletti and A. Farina, "Analysis of Intramuscular electromyogram signals," *Philosophical Transactions of the Royal Society A: Mathematical, Physical and Engineering Sciences*, vol. 367, no. 1887, pp. 357–368, 2009.

Compensatory Tracking Delay Tractability in Closed-loop Dynamic Task based on Visual and Electrotactile Feedback

Hoda Fares[1], Jakob. L Dideriksen[2], Strahinja Dosen[2], Maurizio Valle[1]
[1]Cosmic Lab, DITEN, University of Genoa, Genoa, Italy
[2]Center for Sensory-Motor Interaction, Aalborg University, Denmark

***Abstract*— Latter day hand prostheses lack sensory feedback which impairs close-loop control and embodiment. Providing sensory feedback through electrotactile stimulation has being widely investigated. However, the assessment of tractable time delay and responsive ability of subjects while receiving electrotactile feedback in a dynamic task has rarely tested. The paper studies the compensatory tracking performance while using two different feedback schemes. The reported results demonstrate that tracking using visual feedback enables better control with no delay, while tracking using electrotactile feedback is less susceptible to delays. This in turn, is a good indication for the usability of electrotacile feedback in prosthetic control, since some level of delay is inevitable.**

Keywords: Electrotactile feedback, close-loop control, hand prosthetics, sensory feedback

I. INTRODUCTION

Myoelectric prosthetic hands are usually controlled by recording the electrical activity of user's muscles to estimate motion intention and translate it into commands for the prosthesis. Therefore, they can be used in the restoration of lost motor functions after hand amputation. However this restoration is only partial with absence of comprehensive sensory feedback. Despite the impressive development of prosthesis technologies, there is no hand prosthesis that is even close to replace all of the lost functions. One possibility to improve the user experience is to equip the prosthesis with sensory feedback, thereby closing the control loop. A common method to transmit feedback information is sensory substitution [1]. In this approach, a prosthesis is equipped with sensors measuring system state (e.g., grasping force) and this information is transmitted to the user by delivering tactile stimulation on the skin of the residual limb through vibration motors or electrical stimulation. Electrotactile feedback information can be transmitted by modulating the quality and intensity of the elicited sensations i.e. by changing the stimulation parameters (pulse width, amplitude, and frequency coding) and/or location of the stimulation (spatial coding) [1, 2]. With the ultimate goal of creating a prosthetic system that would compensate for the natural lost limb, by reliably decoding the user's intentions and delivering tactile feedback in a natural manner. This study aims to prove the usability of electrotactile feedback in enabling close-loop control in prosthetics. It evaluates the subject tolerance for different time delays while performing a dynamic control task. In addition, it compares the performance quality of human manual control through a closed-loop compensatory tracking system while using two feedback schemes (i.e. visual and electrotactile feedback). More specifically, this task reflects more accurately the tractable and responsive ability of electrotactile feedback in prosthesis control.

II. Methods

A. Subjects

5 healthy subjects (4 males and 1 female, 30±3 years) participated in two session experiment after signing a consent form under a protocol agreed by the North Denmark Region Committee on Health Research Ethics (N-20160021).

B. Testing setup

A fully programmable multichannel electrotactile stimulator (TremUNA, UNA systems) has been used to deliver electrical stimulation to the subjects. The stimulator is battery powered with eight channels; it generates current-controlled biphasic compensated pluses that range from 0-5mA.Two channels were selected to deliver the stimulation via two self-adhesive concentric electrodes (Spes Medica, 50mm x 50 mm) mounted on the forearm of the dominant hand as shown in fig 1. (a).The pulse width and the intensity for each channel can be adjusted independently, whereas the pulse rate was fixed. In addition, a two DOF joystick (APEM HF22X10U) connected to a PC with USB was utilized to allow the movements along two axes, two

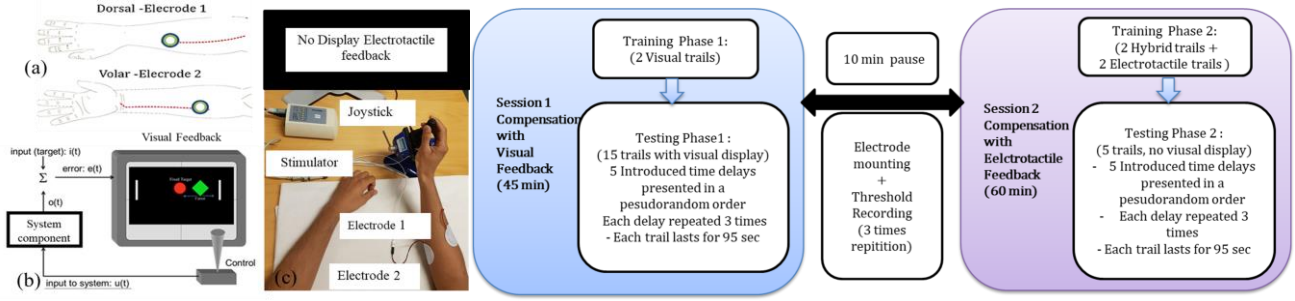

Figure 1: Left: Experimental setup for close-loop compensatory tracking using visual feedback and electrotactile feedback, (a) electrode mounting, (b) compensatory tracking with visual feedback,(c) real photo of tracking with electrotactile feedback. Right: Block diagram of applied testing protocol

movements (either to the right or to the left) were chosen to perform the compensatory track task with visual and electrotactile feedback. A Simulink model developed in MATLAB using a toolbox for closed-loop human manual control [3] was employed to implement the compensatory tracking task. The stimulation parameters were also controlled in real time through the same tool box.

C. *Experimental Procedure and Testing Protocol*

The subject was seated comfortably on a chair in front of table with computer screen in a quite environment. Starting by the experimental task, the subject was asked to track a predefined target trajectory with a control signal that reflected the movement of the joystick in a proportional way. A pseudorandom multi-sine target trajectory was presented for 95 sec in each trail; it was obtained by the summation of 9 sine waves with random phases. Its amplitude was normalized to the range [-0.9, 0.9]. The feedback transmitted to the subject provides the momentary tracking error, which the subject needs to compensate (nullify). Following the testing protocol presented in fig1 the experiment was divided mainly into two testing sessions:

Session 1: *compensation with visual feedback:* The subject was familiarized with the tracking task by providing visual feedback on Pc screen through training phase 1. A green marker deviated from the red vertical line proportionally to the normalized tracking error. If the tracking error reached extreme values of 1 and -1, the marker would hit the limits of the tracking area. The subject was instructed to move the joystick in order to cancel the disturbance (tracking error) and maintain the green marker, as good as possible, at the reference line. To this aim, the subject was supposed to move the joystick in the opposite direction to the movement of the marker proportionally to the magnitude of the deviation (so called position-controlled system). Afterward, the testing phase 1 starts, five time delays (i.e. 0, 0.2, 0.4, 0.8, 1.2 sec) were added to the system and introduced to the subject in pseudorandom order through fifteen trails, while

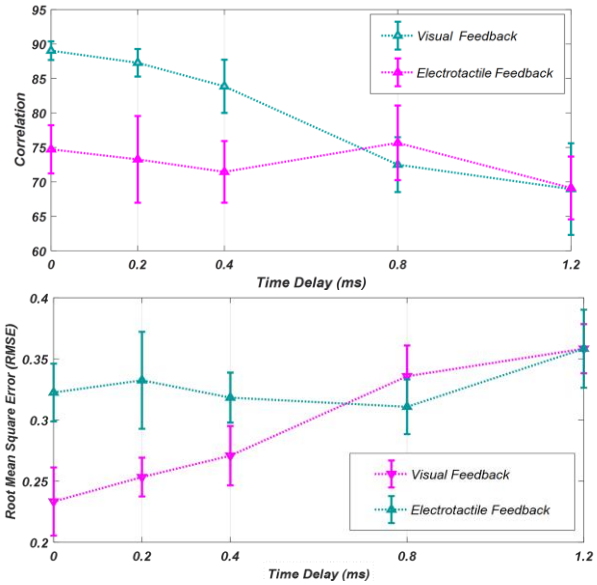

Figure 3: Correlation (top) and Root mean square error (RMSE) (bottom) variation with introduced time delay (ms) across tested subjects visual and electrotactile feedback compensatory tracking.

the subject tracking the error solely using visual feedback. In a following step, the skin of the forearm was cleaned by alcohol wasps and the stimulation electrodes were attached, and then the sensation, discomfort and the pain thresholds were recorded following the method of limits [4]. The pulse width was incremented in steps of 50 us while the frequency and amplitude were set to 70 Hz and 35 mA, respectively. For each electrode, the thresholds recoding has repeated three times and the computed average was used to electro-stimulate the subject.

Session 2*:* Compensation with electrotactile feedback: In the training phase 2, the electrotactile feedback reflecting the tracking error was conducted via the two electrodes simultaneously with the visual feedback aiming to teach the subject to properly interpret the elicited tactile sensation. The two electrodes communicated the sign (electrode) and magnitude (stimulation frequency) of the normalized tracking error. The activation of the electrode positioned on the ventral side of the forearm indicated negative tracking error, while the electrode on the dorsal side signaled positive tracking error. The magnitude of the error was linearly mapped by modulating the frequency of the stimulation. The pulse width was set to 80% of the pain threshold, while the frequency was changed in the range between 7 and 63 Hz. Finally, the subject starts the close-loop tracking using only electrotactile feedback (i.e.no visual display); the same number of trails and delays were tested.

III. Results and Discussion

Two main outcome measures - the correlation coefficient and the root mean square error (RMSE) - were analyzed calculated for each trail at different added time delays for both tracking methods. Figure 3 reports the variation of the average values of correlation and RMSE versus the added time delay in the position control system. The results shows that tracking using visual feedback enables better control with no delay (0 sec), while tracking using electrotactile feedback is less susceptible to delays. This in turn, is a good indication for the usability of electrotacile feedback in prosthetic control, since some level of delay is inevitable.

IV. Conclusion

The paper presented a study of compensatory tracking delay tractability in an online close-loop dynamic task control based while providing visual or electrotactile feedback. It shows the feasibility of using electrotacile feedback for close-loop control of prostheses.

References

[1] "B. Stephens-Fripp, G. Alici, and R. Mutlu, "A review of non-invasive sensory feedback methods for transradial prosthetic hands," IEEE Access, vol. 6, pp. 6878–6899, 2018.

[2] P. Bach-y Rita and S. W. Kercel, "Sensory substitution and the human machine interface," Trends Cogn. Sci., vol. 7, no. 12, pp. 541–546, 2003.

[3] S. Dosen, M. Markovic, C. Hartmann, and D. Farina, "Sensory feedback in prosthetics: a standardized test bench for closed-loop control," IEEE Transactions on Neural Systems and Rehabilitation

[4] N. Prins et al., Psychophysics: a practical introduction. Academic Press, 2016.

Machine and User Co-adaptation in Upper-Limb Myoelectric Control

Dennis Yeung, Dario Farina and Ivan Vujaklija

***Abstract*—A major obstacle to the clinical translation of advanced myocontrol schemes is their reduced reliability due to increased sensitivities to signal perturbations from environmental factors. To that end, adaptive systems that also lend well to users' own adaptation have been proposed to yield more robust systems. Here, a fully unsupervised adaptive system based on Incremental Non-negative Matrix Factorization is presented. The adaptive algorithm, along with its non-adaptive counterparts and a supervised adaptive system, is tested with 12 able-bodied subjects performing virtual target reaching tasks. The experiments were performed in both standard conditions as well as with induced transversal electrode shifts designed to simulate perturbations related to device doffing and donning. While the non-adaptive controllers exhibited statistically significant reductions in performance metrics, both adaptive systems were shown to adequately compensate for the perturbations.**

I. Introduction

RECENTLY, the concept of Simultaneous and Proportional Control (SPC) has been demonstrated to offer intuitive access to multiple degrees-of-freedom (DoF) in myoelectric control applications [1]. While this scheme offers increased functionality over the direct and sequential control schemes employed by most commercial prosthetic devices, it also exhibits increased sensitivity to signal non-stationarities caused by factors such as perspiration, muscle fatigue and electrode displacement [2]. While Hahne et al. demonstrated online system adaptation to improve controller performance [3], the concept of co-adaptation has yet to be tested against signal non-stationarities.

In this work, we propose a fully unsupervised system for online adaptation based on Incremental Non-negative Matrix Factorization (INMF) [4]. The control scheme is tested along with its non-adaptive counterparts, Non-negative Matrix Factorization trained with single-DoF (NMF) [5] and multi-DoF (NMF-C) [6] muscle activations, as well as a supervised online adaptive system based on recursive least squares (RLS-DF) [7].

II. Methods

A. Controller design

The batch initialization of the controller follows the same procedures of conventional NMF where command primitives F is blindly decomposed from training EMG features $\hat{X}$, yielding the latent synergy matrix W:

$$\hat{X} = WF \tag{1}$$

INMF allows for the updating of W as new data x_{t+1} is made available using the following multiplicative update rules:

$$(f_{t+1})_a \leftarrow (f_{t+1})_a \frac{(W_{t+1}^T x_{t+1})_a}{\left(W_{t+1}^T W_{t+1} f_{t+1} + \frac{\beta_1}{2} f_{t+1}^{-\frac{1}{2}}\right)_a} \tag{2}$$

$$(W_{t+1})_{ia} \leftarrow (W_{t+1})_{ia} \frac{(X_t F_t^T + x_{t+1} f_{t+1}^T)_{ia}}{\left(W_{t+1} F_t F_t^T + W_{t+1} f_{t+1} f_{t+1}^T + \frac{\beta_2}{2} W_{t+1}^{-\frac{1}{2}}\right)_{ia}} \tag{3}$$

Where β_1 and β_2 (set as 1 and 7 respectively) tunes the level of sparseness induced in f_{t+1} and W_{t+1} through $L_{1/2}$ regularization. The sufficient statistics of $X_t F_t^T$ and $F_t F_t^T$ are subsequently updated with Equations (4) and (5) where λ, set as 0.995, controls the rate at which past data is discounted.

$$X_{t+1} F_{t+1}^T = \lambda X_t F_t^T + (1-\lambda) x_{t+1} f_{t+1}^T \tag{4}$$

$$F_{t+1} F_{t+1}^T = \lambda F_t F_t^T + (1-\lambda) f_{t+1} f_{t+1}^T \tag{5}$$

This adaptation algorithm is then only triggered during online testing when conflicting commands for the same DoF is issued, signaling a need to update the controller. This is based on the rationale that each DoF should only be activated in one direction at any time. A schematic for this adaptive system is illustrated in Fig. 1.

B. Subjects

Twelve subjects (1 left-handed female and 11 right-handed males, age: 22-31) participated in the experiment with informed consent. The local ethical committee of the Imperial College London (ICREC #18IC4685) approved the study.

C. Data Acquisition

The Myo Armband (Thalmic Labs, Canada), a wireless 8-channel bi-polar EMG recording device which samples at 200Hz was used.

D.Y and I.V. are with the Department of Electrical Engineering and Automation, Aalto University, Espoo, Finland (correspondence to: e-mail: ivan.vujaklija@aalto.fi, +358504707760; dennis.yeung@aalto.fi).

D. F. is with the Department of Bioengineering, Imperial College London, London, UK (e-mail: d.farina@imperial.ac.uk).

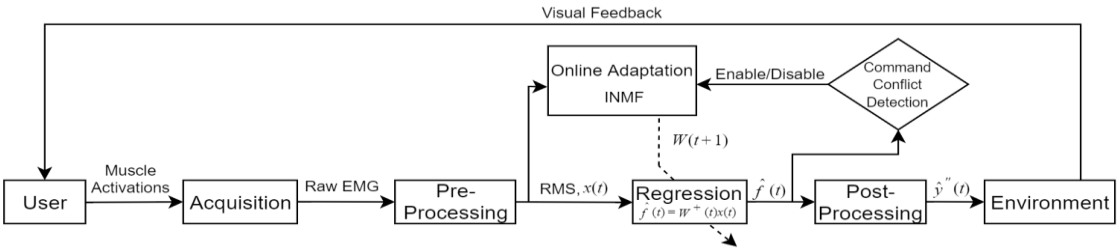

Fig. 1. Schematic of the online estimation and unsupervised adaptation system.

D. Online Testing

During online testing, subjects were asked to perform target hitting exercises in a virtual task-space. This involved maneuvering a cursor where planar displacements (horizontal and vertical) were proportional to estimated wrist movements (flexion/extension and radial/ulnar deviation respectively).

All controllers were tested under normative conditions labelled as "Unshifted". Each evaluation run consisted of 24 targets presented in random order with 10 seconds allowed for each target to be hit. Electrode shifted conditions in both transversal directions "Lateral Shifted" and "Medial Shifted" of 1cm displacement were also tested for all controller types. These shifts represent a 'worst-case' scenario in signal perturbations associated with device doffing/donning and relative movement between the stump and socket.

E. Performance Analysis

Four metrics common to such studies [3], [7]: Completion Rate (CR), Completion Time (CT), Path Efficiency (PE) and Throughput (TP) were used to quantify the performance of each run.

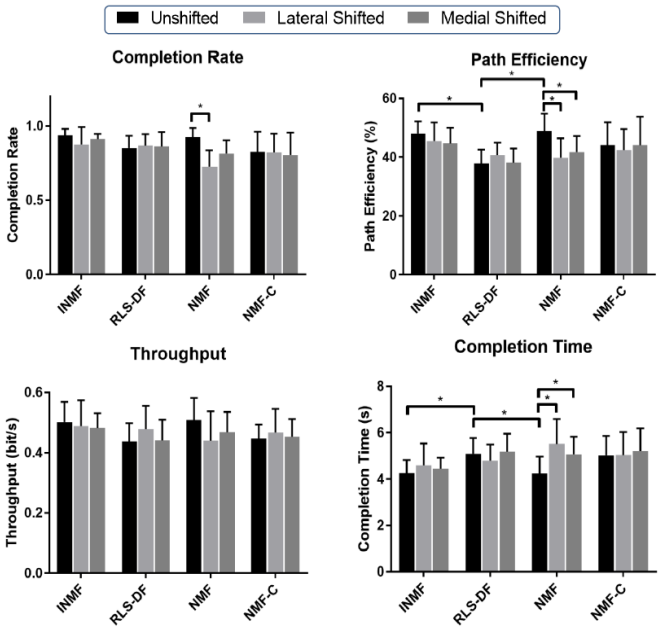

Fig. 2. Performances of co-adaptation with INMF and the supervised RLS-DF compared to pure user-adaptation with NMF and NMF-C when compensating for transversal electrode shifts.

III. Results and Discussion

From two-way RM-ANOVA, significant interaction between algorithm and electrode shift was detected in the metrics of CR (p=0.011), PE (p=0.017) and CT (p=0.012) and results can be seen in Fig. 2. From focused ANOVA fixed on NMF, CR was lower in Lateral Shifted compared to Unshifted (-0.20, ±0.05, p=0.001). For PE, Unshifted was significantly higher than both Lateral Shifted (+9.16, ±2.37%, p=0.008) and Medial Shifted (+7.96, ±1.96%, p=0.011). CT for NMF in Unshifted was also found lower than both Lateral Shifted (-1.28, ±0.02s, p=0.016) and Medial Shifted (-0.824, ±0.046s, p=0.046).

In summary, control with NMF was significantly deteriorated by the electrode shifts and user-adaptation alone was insufficient for recovering. Conversely, NMF-C was less affected by the shifts, however, its baseline performance was lower due to a less intuitive mapping. Meanwhile, both co-adaptive systems were able to compensate for the shifts, reinforcing the notion that concurrent adaptation of user and system can yield superior robustness. In the case of INMF, its unsupervised nature may lend itself well to clinical scenarios where system adaptation occurs on-demand without requiring any external input.

References

[1] Ning Jiang, S. Dosen, K.-R. Muller, and D. Farina, "Myoelectric Control of Artificial Limbs—Is There a Need to Change Focus? [In the Spotlight]," *IEEE Signal Process. Mag.*, vol. 29, no. 5, pp. 152–150, Sep. 2012.

[2] D. Farina *et al.*, "The extraction of neural information from the surface EMG for the control of upper-limb prostheses: Emerging avenues and challenges," *IEEE Trans. Neural Syst. Rehabil. Eng.*, vol. 22, no. 4, pp. 797–809, Jul. 2014.

[3] J. M. Hahne, S. Dahne, H.-J. Hwang, K.-R. Muller, and L. C. Parra, "Concurrent Adaptation of Human and Machine Improves Simultaneous and Proportional Myoelectric Control," *IEEE Trans. Neural Syst. Rehabil. Eng.*, vol. 23, no. 4, pp. 618–627, Jul. 2015.

[4] S. S. Bucak and B. Gunsel, "Incremental subspace learning via non-negative matrix factorization," *Pattern Recognit.*, vol. 42, no. 5, pp. 788–797, May 2009.

[5] N. Jiang, H. Rehbaum, I. Vujaklija, B. Graimann, and D. Farina, "Intuitive, Online, Simultaneous, and Proportional Myoelectric Control Over Two Degrees-of-Freedom in Upper Limb Amputees," *IEEE Trans. Neural Syst. Rehabil. Eng.*, vol. 22, no. 3, pp. 501–510, May 2014.

[6] D. Yeung, D. Farina, and I. Vujaklija, "Can Multi-DoF Training Improve Robustness of Muscle Synergy Inspired Myocontrollers?," in *2019 IEEE 16th International Conference on Rehabilitation Robotics (ICORR)*, 2019, pp. 665–670.

[7] D. Yeung, D. Farina, and I. Vujaklija, "Directional Forgetting for Stable Co-Adaptation in Myoelectric Control," *Sensors*, vol. 19, no. 9, p. 2203, May 2019.

The use of a Brain Computer Interface (BCI) in Gait Rehabilitation of Stroke Patients

Juan Vázquez-Díez, Aitor Martínez-Expósito, Alberto Montalva-Iborra, Enrique Viosca-Herrero and José L. Pons

***Abstract*— With the aid of a BCI we will synchronize afferent and efferent signals in chronic stroke patients in order to mimic physiological mechanisms and potentiate neural pathways involved in locomotion. Clinical measures as well as corticospinal excitability will be tested prior to the intervention and after it to prove its short-term efficacy in the rehabilitation of gait. We present an overview of the research plan based on the pilot study results.**

I. Introduction

STROKE , one of the most frequent sources of disability, has an estimated incidence of 150/100,000 inhabitants per year, 30-40% of which will present invalidating sequelae [1]. It may affect a wide variety of body functions, including walking capacity. Improvement of function will be seen mainly in the first 3 months [1], and it may extend further up to 6 months. After that, mild improvements in function can appear, but they will most likely lack clinical significance. Short-term improvement is due to the reperfusion of the ischemic penumbra while long-term improvement (usually scarce) will be due to neuroplasticity.

Even though little improvement in strength is usually seen in patients with stroke, motor control training and adaptations can improve function and participation of the patient, exceeding what would be expected if only strength was taken into account. Rehabilitation is the specialty that will enable the achievement of these goals through specific training programs. However, current neurorehabilitation treatment for stroke patients is time-consuming and results are suboptimal if a complete recovery is aimed. In these rehabilitation programs, patients perform passive and active movements as well as proprioceptive exercises hoping that these will restore normal motor patterns.

A current and novel approach to neurorehabilitation is the ability to potentiate neuroplasticity through correct timing of interventions. This is achieved through brain-computer interfacing. In this approach, there is a volitional motor intention that the patient performs trying to move the affected limb (top-down approach) as well as sensory information (mainly proprioceptive) that is sent from the affected limb to the brain (bottom-up approach). It has been demonstrated that, if these two signals are precisely timed, neuroplasticity may be enhanced beyond what current rehabilitation programs are able to achieve and this may translate into better walking performance [2], [3].

During gait, preferred walking speed coincides with minimal energy expenditure since the person is taking full advantage of passive forces (gravity and elasticity of lower limb soft tissue) to maintain walking speed. Energy usage increases both at lower and higher-than-preferred speeds. Lower limb muscles can be classified into two main groups depending on their overall function in gait: 1. restoration of spring torque (regarding lower limb elasticity), and 2. restoration of energy lost in each stride. The first group comprises proximal lower limb muscles (quadriceps and ischiotibial muscles) and are in charge of modulating walking cadence and hence speed, while the second group includes distal lower limb muscles (mainly tibialis anterior, gastrocnemius and soleus) [4].

II. Aim

The aim of our study is to confirm in a larger population of chronic stroke patients the increase in corticospinal excitability after a training session using a BCI to couple the movement-related cortical potential (MRCP) with the FES stimulation on quadriceps, as well as to quantify the clinical implications of such treatment, taking into account the results obtained in the feasibility study [5].

III. Material and Methods

A. Patients

We will recruit chronic lacunar stroke patients from those who attend our hospital who present some degree of hemiparesis (lower limb clinically detectable involvement is mandatory), but who are able to walk. All patients will fulfill requirements determined by the study clinicians, which have been previously approved by the hospital's ethics commitee.

This project has received funding from the Ministry of Economy (MINECO) of Spain and is part of the Associate Consortium (799158449-58449-45-514).

J. Vázquez-Díez, E. Viosca-Herrero and A. Montalva-Iborra authors are with Insituto de Investigación Sanitaria La Fe, Valencia, Spain (corresponding author e-mail: vazquez_juadie@gva.es).

A. Martínez-Expósito and J.L. Pons authors are with the Neural Rehabilitation Group of the Spanish National Research Council, Madrid, Spain.

B. *TMS assessment*

Corticospinal excitability will be used as a measure to determine synaptic enhancement and therefore the potential to induce neuroplasticity. It will be determined by generating and quantifying motor evoked potentials (MEP) through the use of single-pulse transcranial magnetic stimulation (TMS) and surface electromyography (sEMG) on rectus femoris, biceps femoris, tibialis anterior and soleus as shown in fig. 1. This procedure is performed before, immediately after and 30 minutes after the training session with the BCI.

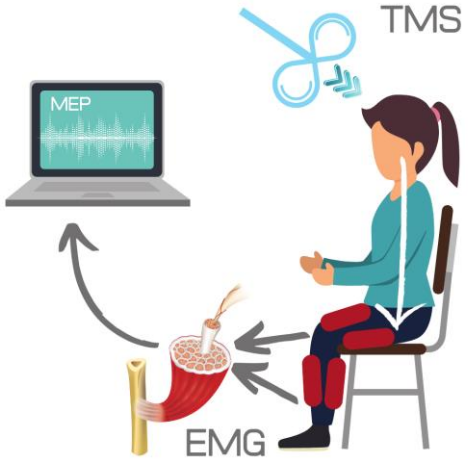

Fig. 1. TMS assessment setup and procedure overview.

C. *Clinical assessment*

Assessment for clinical outcomes will be performed using both objective biomechanical measures as well as through clinical evaluation scales, both for balance and gait performance. Overall independence will be determined by means of the Barthel Index.

D. *Brain-computer interface*

The BCI will be calibrated to detect MRCPs by means of surface EEG when the patient is asked by means of a visual cue to initiate a volitional lower limb cycling movement. Functional electrical stimulation (FES) over rectus femoris, which is one of the main muscles involved in walking speed, will be timely activated with a predefined delay to the detected MRCP in order to assist the cycling movement. This will hopefully reinforce synaptic connections and therefore enhance neuroplasticity through induced proprioception (due to movement derived from timely FES activation). Fig. 2 outlines the BCI setup.

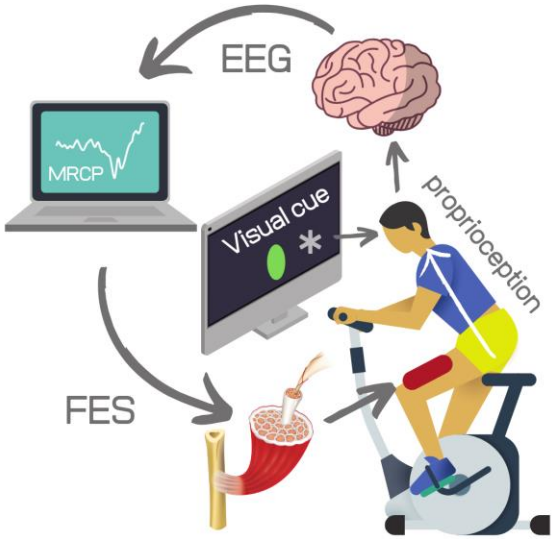

Fig. 2. BCI setup and procedure overview. Initial step is marked with "*".

IV. Discussion

Gait disturbance greatly affects stroke patients' quality of life and participation in daily activities. Current neurorehabilitation treatments lack integration of both the bottom-up and top-down approaches, meaning that we are probably missing a neuroplasticity enhancement opportunity that could improve treatment outcomes. By means of a BCI we will be able to couple motor intention (MRCP) with FES and hopefully enhance neuroplasticity beyond what is being achieved with current rehabilitation programs. However, it is not clear whether this neuroplasticity will suffice to increase walking speed and/or improve overall function and participation. We will perform clinical validation of this platform in order to determine its utility in stroke patients regarding walking and balance function as well as independence.

References

[1] Á. A. Cuadrado, "Rehabilitación del ACV. Evaluación, pronostico y tratamiento," vol. 70, no. 3, pp. 25–40, 2009.

[2] N. Mrachacz-Kersting *et al.*, "Efficient neuroplasticity induction in chronic stroke patients by an associative brain-computer interface," *J. Neurophysiol.*, vol. 115, no. 3, pp. 1410–1421, Mar. 2016.

[3] E. Ambrosini, S. Ferrante, A. Pedrocchi, G. Ferrigno, and F. Molteni, "Cycling induced by electrical stimulation improves motor recovery in postacute hemiparetic patients: A randomized controlled trial," *Stroke*, vol. 42, no. 4, pp. 1068–1073, 2011.

[4] D. M. Russell and D. T. Apatoczky, "Walking at the preferred stride frequency minimizes muscle activity," *Gait Posture*, vol. 45, pp. 181–186, 2016.

[5] A. Martínez-Expósito, J. Vázquez-Díez, J. Ibáñez, E. Viosca, and J. L. Pons, "Brain activity dependent neuroprosthetic for cycling task in stroke patients: Feasibility study," in *School and Symposium on Advanced Neurorehabilitation (SSNR2018)*, 2018, pp. 5–6.

Pilot Study: Investigating the Impact of Adult Spinal Deformity Surgery on Overground Walking

Karley E. Benoff, Maximilian Walter, Hannah J. Weaver, and Rajiv Saigal

***Abstract*—Motion capture technology provides dynamic quantitative assessments of movement that can supplement clinical and rehabilitative decision making. Although widely used for some pathologies, dynamic analyses infrequently report the heterogeneous population of adults with spinal deformities. We have conducted a pilot study with a single recipient of adult spinal deformity surgery to investigate how surgery impacts walking ability and quality of life as monitored clinically. As hypothesized, we found that postoperatively, the participant had a more stable and normative gait pattern in comparison to their preoperative analysis. This study is actively recruiting participants to evaluate a larger cohort of individual gait patterns and additional dynamic movements as compared to age-gender matched healthy controls.**

I. Introduction

ADULT spinal deformity (ASD) is a heterogeneous condition defined by a lack of spinal alignment often associated with discomfort and altered mobility. When deformity surgery is appropriate, the current standard of care is to use static, radiographic-based assessment of spinopelvic parameters and patient-reported outcomes (PROs) for surgical planning [1]. However, these methods do not capture dynamic postural changes that could be more representative of daily living and more informative for individualized care.

Recently, prior literature on ASD has sought to quantify dynamic movement pre- and postoperatively using various motion capture technologies for over-ground walking and a sit-to-stand task [2-5]. Despite the potential these analyses have to compliment surgical and rehabilitative planning for ASD, there is a paucity of information elucidating dynamic information like kinematics; in comparison, adjacent pathologies like adolescent scoliosis have been studied using motion analysis techniques for decades [5-6]. Future ASD surgical and rehabilitative planning may incorporate dynamic analyses, but significant translational barriers exist for adoption beyond academic research; most prominently, these include the lack of correlations with relevant clinical metrics and the sparsity of published longitudinal studies [6].

This research has been funded by the University of Washington Amplifying Movement & Performance (AMP) Lab and the University of Washington Department of Neurological Surgery.

K. E. Benoff is with the Departments of Mechanical Engineering and Neurological Surgery of the University of Washington, Seattle, WA, United States (email: kbenoff@uw.edu).

R. Saigal, is with the Departments of Neurological Surgery and Bioengineering of the University of Washington, Seattle, WA, United States (email: rsaigal@uw.edu)

The purpose of this pilot study is to compare lower-limb kinematics and spatiotemporal metrics of an individual with ASD pre- and postoperatively. Dynamic differences were also analyzed for correlations with relevant clinical PROs. This preliminary work will aid further advancements into novel dynamic movements within this patient population and comparisons with age-gender matched healthy individuals for a larger cohort of study participants.

II. Methods

One individual with clinical indications of adult spinal deformity (preoperative: 61 yrs, 1.68 m, 91 kg; postoperative: 61 yrs, 1.65 m, 83 kg) was recruited for this pilot study. The subject gave their informed consent prior to participating in the study.

The participant attended two lab sessions for collection of kinematic, kinetic, and biometric data. The first session was held preoperatively during the same week as their surgery; the second session was held three months postoperatively. Forty-three retro-reflective markers were placed using a modified Plug-In-Gait model. For each session, the participant was instructed to walk at a self-selected speed along an approximately 15-meter path containing four force plates (Kistler, Novi, Michigan, United States). Ten Qualisys motion capture cameras (Qualisys, Göteborg Sweden) recorded marker positions. For each session, a minimum of 10 walking trials were collected, defined by one pass through the path.

A. Calculations

Reflective marker positions were extracted from Qualisys Track Manager and joint ranges of motion were calculated in OpenSim version 3.3 using standard inverse kinematics techniques [7]. This information was exported into a custom MATLAB script to calculate spatiotemporal metrics including step width, step length, and average speed, and kinematics for the lower limbs. Step width and step length are defined by the difference in lateral malleolus marker positions as projected on the coronal and sagittal planes, respectively. Gait speed is defined as the displacement over time of the sternal junction marker between the first and last heel strike per trial. Kinematic curves were normalized from heel strike to heel strike of a single leg.

III. Results and Discussion

Compared to preoperative, postoperative spatiotemporal parameters and knee kinematics trended towards normative

values [8]. Step width decreased by 13.8%, step length increased by 8.1%, and average gait speed increased by 11.8% (Table I). These changes indicate that the participant's postoperative gait showed improved stability, consistent with previous literature [2].

TABLE I
SUMMARY OF SPATIOTEMPORAL PARAMETERS

Parameter	Preoperative	Postoperative
Step Width	24.7 ± 3.7 cm	21.3 ± 3.0 cm
Step Length	49.2 ± 2.9 cm	53.2 ± 3.1 cm
Gait Speed	93.3 cm/s	104.3 cm/s

For individuals with ASD, positive sagittal balance, or when the C7 vertebrae remains anterior to the S1 vertebral segment, is common. To compensate for this forward torso lean, many individuals, including the pilot participant, have increased knee flexion while standing and walking; this can be seen by the increased duration of maximal flexion during the gait cycle (Fig. 1). Postoperatively, the average knee range of motion increased by 10.2º and decreased in width to a more normative, bimodal curve. We are currently performing statistical analyses to determine statistical significance of these changes.

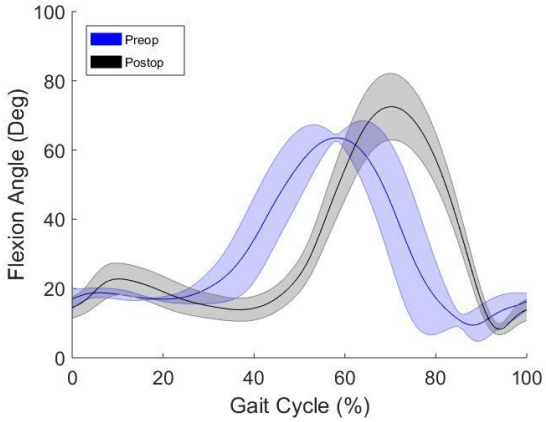

Fig. 1. Kinematic curves of the knees normalized by gait cycle, defined as heel strike to heel strike of one limb. The solid line indicates an average value with one standard deviation shaded above and below. Preoperative values are in blue and postoperative values are in black.

A. *On-Going Trials*

This study is actively recruiting patients within the University of Washington Medical System. The results from this preliminary investigation will be used to inform future data collection methods and to expand analyses for a broader range of movement tasks.

IV. CONCLUSION

To our knowledge, the dynamic movement of individuals with ASD is still relatively uncharacterized; Given the inherent heterogeneity of this patient population, there is a present need for more motion capture-based analyses if the future of clinical interventions and rehabilitation are to advance beyond static radiography. This preliminary work aims to contribute to a greater body of information which holds promise to advance clinical and rehabilitative care for ASD to improve patient quality of life.

ACKNOWLEDGMENT

This study was financially supported by the University of Washington Amplifying Movement & Performance (AMP) Lab and the University of Washington Department of Neurological Surgery.

REFERENCES

[1] C.P Ames, J.K.Scheer, V. Lafage, J.B. Smith, S. Bess, B.H. Berven, et al. "Adult spinal deformity: epidemiology, health impact, evaluation, and management". Spine Deform vol 4, 2016, pp. 310-322

[2] J.R. Engsberg, K.H. Bridwell, J.M. Wagner, M.L. Uhrich, K. Blanke, L.G. Lenke. "Gait Changes as the result of deformity reconstruction surgery in a group of adults with lumbar scoliosis". Spine vol 28, Aug 2003, pp. 1836-1844

[3] J.F. Bailey, R.P. Matthew, S. Seko, P. Curran, L. Chu, S.H. Berven, et al. "Biomechanical changes in dynamic sagittal balance and lower limb compensatory strategies following realignment surgery in adult spinal deformity patients". Euro Spine J. 201, pp 1-9

[4] M. Yagi, H. Ohne, T. Konomi, K. Fujiyoshi, S. Kaneko, M. Takemitsu, M. Machida, Y. Yato, T. Asazuma. "Walking balance and compensatory gait mechanisms in surgically treated patients with adult spinal deformity". Spine J vol 3. Mar 2017, pp 409-17

[5] B.G. Diebo, N.V. Shah, R. Pivec, A. Naziri, N.H. Post, A. Assi, et al. "From static spinal alignment to dynamic body balance: utilizing motion analysis in spinal deformity surgery". JBJS Rev 7, e3, 2018

[6] K.W. Wu, J.D. Li, H.P. Huang, Y.H. Liu, T.M Wang, Y.T. Ho, T.W Lu. "Bilateral asymmetry in kinematic strategies for obstacle-crossing in adolescents with severe idiopathic thoracic scoliosis". Gait & Posture vol 7. Apr 2019. pp 211-218

[7] S.L Delp., F.C. Anderson, A.S Arnold, P. Loan, A. Habib, C.T. John, et al. "OpenSim: Open-source software to create and analyze dynamic simulations of movement". IEEE Transactions on Biomedical Engineering vol 55, 2007. pp 1940-1950.

[8] T. Oberg, A. Karszania, K. Oberg. "Basic gait parameters: reference data for normal subjects", 10-79 years of age. J Rehabil Res Dev vol 2, 1993, pp 210-23

Initial Design Considerations for an Adaptive Functional Electrical Stimulation System

First A. V. Nandakumar, Second B. I. Swain, Third C. P. Taylor and Fourth D. E. Merson

***Abstract*—Functional Electrical Stimulation (FES) is a rehabilitation method that is being used to treat people with neurological disorders. The FES device makes use of electrical stimulation to activate muscles that are dysfunctional due to these neurological problems and is commonly used to treat drop foot. Initially, with the aid of a questionnaire one of the areas of concern for the device users were found to be walking on varied terrains and obstacles. This paper provides the initial design for an FES device that aims to adapt to different walking scenarios. The design will suggest the use of various sensors to detect the terrain and a closed-loop control system to adapt stimulation parameters in response to variation in terrains. It is expected that this design will allow the current device users to walk more confidently with less fear in different terrains.**

I. Introduction

FUNCTIONAL Electrical Stimulation (FES) is an established technique used in people with central neurological dysfunctions like Multiple Sclerosis, stroke, incomplete spinal cord injury, etc. FES devices make use of electrical nerve stimulation to produce useful muscle contraction to elicit everyday functional movements in these people. These muscle contractions are produced by placing surface electrodes over the nerves and by providing electrical pulses. This neuroprosthetic device is frequently used to assist walking by treating a condition called Drop Foot (DF), a result of paralysis of the pretibial muscles [1]. DF is an inability to lift the foot, reducing the control of the foot during walking and inducing instability during gait in individuals with central neurological damage [2]. FES devices treat DF by stimulating the common peroneal nerve causing the foot to lift as required and provide floor clearance during the swing phase of gait [3].

All the well-known commercial Drop Foot Stimulators (DFS) such as the Odstock DFS [4], Walkaide stimulators [5], Actigait system [6], STIMuSTEP [7] and the Bioness L300 have been shown to help improve mobility significantly. Yet there are some areas which require improvement [8].Variation in stimulation parameter control is a possible method to improve its functional outcome. Likewise, all the current systems have constant pre-set stimulation parameters such as constant current, pulse width, frequency, etc. [9]. These parameters are always optimized to walk on level ground rather than for different walking scenarios as stairs, slopes, and uneven pavements. Fig. 1 shows the main working principle of FES.

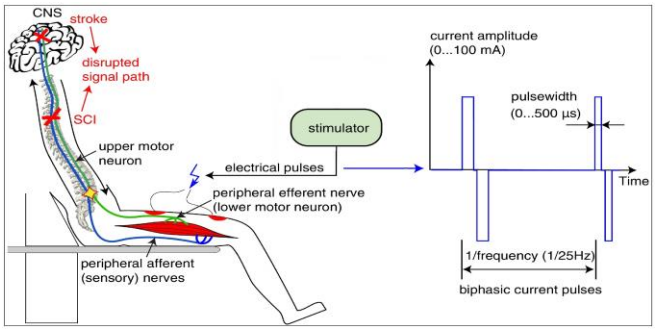

Fig. 1. Principle FES working [8].

Similarly, research proposes that 'Real–world FES applications require the ability to modulate the pulse-to-pulse electrical stimulation in real-time to compensate for fatigue, muscle spasms, retraining effects, modeling errors and exogenous disturbances. Closed loop control system can be used to address these challenges' effectively [10]. Some of the currently used closed loop control strategies are fuzzy logic, neural network, adaptive sliding mode, proportional-integral-derivative and adaptive controllers [11].

Sensors are another important part of an FES system; they provide the essential feedback to the control system in order to be able to perform the controlling effectively. Pressure sensors are used as foot switches to control the stimulation in many of the current FES devices [12]. Other devices employ accelerometers, gyroscopes and Inertial Measurement Units (IMU) in their system [13]. This research proposes an idea to design an adaptive FES device with the help of suitable sensors and control system. This new system will be able to modulate the stimulation parameters and make it suitable for the users to walk on different walking scenarios.

This Ph.D. project is match funded by Bournemouth University and Odstock Medical Limited.

F. A. Author is with the Faculty of Science and Technology, Bournemouth University and Odstock Medical Limited, Salisbury, United Kingdom (vnandakumar@bournemouth.ac.uk).

S. B. Author is with the Faculty of Science and Technology and Faculty of Health and Social Science, Bournemouth University, Bournemouth, United Kingdom (iswain@bournemouth.ac.uk).

T. C. Author is with the Faculty of Health and Social Science, Bournemouth University and Odstock Medical Limited, Salisbury, United Kingdom (Paul.Taylor@odstockmedical.com).

F. D. Author is with the Faculty of Science and Technology, Bournemouth University and Odstock Medical Limited, Salisbury, United Kingdom (Earl.Merson@odstockmedical.com).

II. Proposed Method

At the initial stage of this research we administered a questionnaire to 29 patients (age SD- 11.3) with DF, from the National Clinical FES Centre, at Salisbury District Hospital (UK). All the recruited patients had used the ODFS for at least 6 weeks prior to the survey. The survey was carried out to understand the usage and limitations of the current FES devices from the user's perspective. The questions explored how the device performed while the individual walked on different surfaces and obstacles, for instance, while climbing the stairs, or when walking on uneven pavements with the DFS [14]. The responses showed which terrains caused difficulty and some of these terrains were chosen to be detected in this project.

As the next stage of the project, a sensor module will be developed, which will be used to detect some terrains resolved earlier from the questionnaire results. The various walking scenarios were chosen based on the frequency of encountering it in daily life and the effort required by the user to tackle it. The sensor module is expected to measure some aspects of the user's gait to distinguish the terrain the user walks on. The output of this sensor-based system will then provide feedback to the control system. Then this controls the DFS and will vary the stimulation parameters as required for each walking scenario.

III. Results

The responses to the questionnaire showed the perspective of the participants about walking on different terrains and obstacles. Table I shows the percentage of participants who were able and unable to access stairs, ramps, and kerbs with and without the stimulator.

TABLE I
Participant's accessibility of stairs, ramps and kerbs [14]

	Cannot Access (with/without DFS)	**Can only Ascend (with DFS)**	**Can only Descend (with DFS)**	**Can Ascend and Descend (with DFS)**
Stairs	22%	3%	3%	72%
Ramps	21%	7%	3%	69%
Kerbs	17%	0	0	83%

According to this data, a substantial number of the survey volunteers were able to access these obstacles only with the help of the stimulator. When asked to explain their experience, many users said, even with the DFS they followed certain gait patterns to overcome these obstacles.

Similarly, all the participants rated the effort required to walk on different terrains on a Likert scale of 1-5 where 1was effortless and 5 was a great effort as shown in Fig. 2. From these results, we observed that cobbled street was the most difficult terrain to walk on. 28% of the participants stated so due to the unevenness of the surface, which required more effort to clear the ground without tripping.

Contrastingly, carpets were the easiest surface to walk on. 34% said it was easy to walk on carpets as they were not very varied to level ground demanding no change in gait patterns. Additionally many participants highlighted that gravel and pavements were the most common terrains they encountered, which also required more effort than required to walk on level ground.

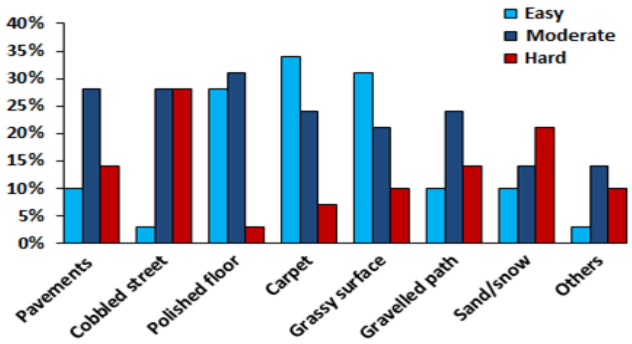

Fig. 2. Participant's Likert scale rated effort to walk on different terrains [14].

IV. Discussion and Conclusions

The result shows us that in spite of using the DFS, many participants required great effort to overcome most of the terrains. Some even said they followed special gait patterns to do so, such as descending the stairs by coming down backward or sideways, initially progressing with the unaffected leg, circumduction of the hip, dragging their foot and other abnormal ground clearing methods. Accessing these obstacles becomes even more demanding or even impossible for individuals who are bilaterally affected.

More than 20% of the survey respondents said that the main problem they faced in most of these terrains was the inadequacy of foot lift that was required to clear the floor on certain surfaces. Hence, it is predicted this could be a result of having to tackle different walking scenarios with the same stimulation parameters that are usually set to walk on level ground when the user comes to the clinic. Thus, this project suggests an idea to develop an FES system with suitable sensors to provide feedback to the closed-loop control system. It is expected this adaptive system would make it more reliable for the user and allow them to walk more confidently in different terrains and obstacles. The paper enumerates the early-stage ideas of the project in designing an FES device that could be adaptive to various walking scenarios.

REFERENCES

[1] L. L. Baker, D. R. McNeal, L.A. Benton, B. R. Bowman, and R. L. Waters, *NeuroMuscular Electrical Simulation- A Practical Guide*. 3rd edition, Ed. Los Amigos Research and Education Institute, 1993, ch. 9.

[2] M. Chen, et al., "A self-adaptive foot-drop corrector using Functional Electrical Stimulation (FES) modulated by tibialis anterior electromyography (EMG) dataset," *Medical Engineering & Physics*, 35(2), 2013, pp. 195-204.

[3] B. Singer, "Functional Electrical Stimulation of the extremities in the neurological patient: A review," *Australian Journal of Physiotherapy*, 33(1), 1987, pp. 33-42.

[4] J. Burridge, P. Taylor, S. Hagan, and I. Swain, "Experience of clinical use of the Odstock dropped foot stimulator," *Artif Organs*, 21(3), 1997, pp. 254-260.

[5] J. Robertson and M. Whittaker, “Clinical perspectives in fitting the WalkAide2 foot-drop stimulator,” *10th Annu. Conf. Int. FES Soc*., 2005, pp. 6–8.

[6] K. D. Martin, et al., “ActiGait implantable drop foot stimulator in multiple sclerosis: A new indication,” *J Neurosurg.*, 126(5), 2017, pp. 1685-1690.

[7] P. N. Taylor, I. A. W. Hart, M. S. Khan, and D. E. M. Slade-Sharman, “Correction of footdrop due to multiple sclerosis using the STIMuSTEP implanted dropped foot stimulator,” *Int J MS Care*, 18(5), 2016, pp. 239-247.

[8] T. Schauer, “Sensing motion and muscle activity for feedback control of functional electrical stimulation: Ten years of experience in Berlin,” *Annual Reviews in Control*, 44, 2017, pp. 355-374.

[9] A. B. Hmed, T. Bakir, S. Binczak, and A. Sakly, “Model free control for muscular force by functional electrical stimulation using pulse width modulation,” *Control Engineering & Information Technology (CEIT) 2016 4th International Conference*, 2016.

[10] C. Lynch and M. Popovic, “A comparison of closed-loop control algorithms for regulating electrically stimulated knee movements in individuals with spinal cord injury,” *IEEE Trans Neural Syst Rehabil Eng.*, 20(4), 2012, pp. 539–548.

[11] A. D. Koutsou, J. C. Moreno, A. J. del Ama, E. Rocon, and J. L. Pons, 2016. “Advances in selective activation of muscles for non-invasive motor neuroprostheses,” *J. Neuroeng. Rehabil*, 13, 2016, pp. 56.

[12] G. Chen, L. Ma, R. Song, L. Li, X. Wang, and K. Tong, “Speed-adaptive control of functional electrical stimulation for dropfoot correction,” *J. Neuroeng. Rehabil*, 15, 2018, pp. 98.

[13] L. Meng, B. Porr, and H. Gollee, “Technical developments of functional electrical stimulation to restore gait functions: Sensing, control strategies and current commercial systems,” *Chinese Journal of Scientific Instrument*, 6, 2017, pp. 1319-1334.

[14] V. Nandakumar, I. Swain, P. Taylor, and E. Merson, “Analysing the performance of Odstock drop foot stimulator in different walking scenarios: A survey research,” unpublished.

Motor synergies of cyclic upper limb movement

Lilla Botzheim, Szabolcs Malik, József Laczkó

***Abstract*—The number of potentially controlled muscle synergies in bimanual arm cycling movements is studied. Earlier we examined muscle synergies in 4D muscle spaces for the dominant and non-dominant arms separately using non negative matrix factorization. Here we study the two arms together during upper limb cycling on cycle-ergometers in which the two handles of the device were connected and also when the handles (the left and right cranks) were physically not connected. Beside one-sided synergies we studied muscle synergies in 8D muscle space that is defined by muscles from both arms. It was found that a) the synergies extracted in the dominant and non-dominant arms separately were similar b) the synergies extracted from the two arms together, indicated that the investigated movement was bimanual.**

I. Introduction

In this study, we investigated the connection between the motor symmetry and the motor synergy revealed in bimanual arm cranking movements. Two experiments were designed, during which able bodied participants performed arm cranking movement on arm cycle ergometers. Muscle activities (EMG) of four muscles were recorded in each arm. The synergies were calculated in the 4D muscle space when only one arm (and its four muscles) was considered (one-sided synergy). Synergies were also calculated in the 8D muscle space when both arms (and its eight muscles) were considered (two-sided synergy). Non-negative matrix factorization (NMF) method was applied to extract synergies from recorded muscle activities (time series of EMG signals). We approximated 4D muscle activity vectors by linear combination of 2 synergies in the one-sided cases, and 8D muscle activity vectors by 2 synergies and by 4 synergies in the two-sided case. There were two main questions. Q1: Can two-sided (8D) synergies assembled from 2 one-sided (4D) synergies? Q2: Do two-sided synergies show that they relate to bimanual movements?

II. METHODS

A. Experimental setup

In the first experiment, participants performed arm cranking on an arm cycle ergometer (Meyra, Germany). They cranked in anti-phase cycling mode with both arms for 30 seconds guided by a metronome. The ergometer's handles were connected. In the second experiment, the participants executed the arm cranking task on a custom designed device, which handles were unconnected. (Figure 1) On this device, participants cranked also with both arms in anti-phase mode. During the two measurements, we recorded the activity (EMG) of eight muscles, biceps, triceps, anterior deltoid and posterior deltoid from both arms. We filtered the raw EMG data with 4^{th} order, bandpass Butterworth filter and smoothed the EMG signals applying root mean square (RMS) method with 88ms window width. The data of the second experiment (cranking on a custom designed device) were normalized by maximum values and their envelope were calculated as it was proposed by other studies. [1,2,3]

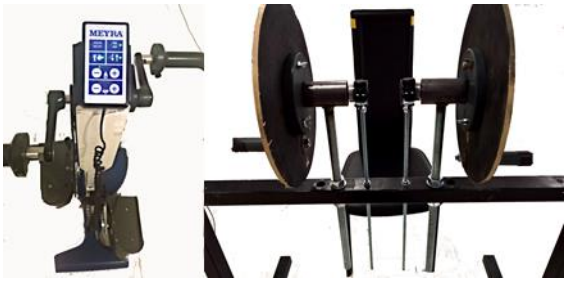

1. Figure First device is the Meyra ergometer with connected handles. The second is the custom designed device with unconnected handles

B. Computation

Dimension reduction methods (non-negative matrix factorization) was applied to extract muscle synergies. We approximated the activity patterns of four muscles (4-dimensional vectors as function of time) of each arm by linear combination of 2 synergies (4D one-sided synergies for the left and the right arm separately). We approximated the activity patterns of eight muscles (8 dimensional vectors as function of time) involving both arms by linear combination of 2 synergies (8D two-sided synergies). 8D muscle activities were approximated (reconstructed) by 4 synergies too. The mean synergy vectors across participants were calculated for all cases. The synergies reflect the compressibility of the data, which was characterized by muscle activity variances accounted for (VAF) by a given number of synergies. Therefore, the VAF values were also computed, evaluated and averaged across participants.

III. Results

In one-sided case the muscle activity pattern in 4D was reconstructed by 2 synergies and in two-sided case the muscle activity pattern in 8D was reconstructed by 2 synergies and by 4 synergies. The VAF value was over 95% for both arms when the right and left arm was considered separately. These results may reflect a symmetric property of this cyclic movement task. The VAF value for 2 synergies of 8D muscle activity was over 90%, and for 4 synergies VAF was over 97% (Table I.).

Supported by grants GINOP 2.3.2-15-2016-00022 and KAP19-12003-1.1-ITK

Lilla Botzheim is with the Wigner Research Centre for Physics, Budapest, Hungary and the University of Pecs, Pecs, Hungary (corresponding author to provide e-mail: botzheim.lilla@wigner.mta.hu).

Malik Szabolcs is with the Wigner Research Centre for Physics, Budapest, Hungary.

József Laczkó is with the Wigner Research Centre for Physics, Budapest, Hungary and the University of Pecs, Pecs, Hungary

TABLE I.

Conditions	VAF values			
	two-sided synergies		one-sided synergies	
	2 Syn 8D	4 Syn 8D	2 Syn 4D left	2 Syn 4D right
Connect	90,8%	97,5%	95,3%	95,9%
Unconnect	94,2%	99,0%	98,6%	98,4%

One-sided synergies were compared. We used the normalized scalar product for characterizing similarity.[4] Synergy1 in left arm and synergy1 in right arm were similar and we found the same in synergy 2. (Figure 2). This was found in the case when the left and right handle of the device were connected and also in that case in which the handles were not connected (Table II).

TABLE II.

Conditions	one-sided synergies	
	synergy1	synergy2
Connect	0.9747	0.9677
Unconnect	0.9542	0.9843

This finding also reflects symmetry of the movement task. We compared the 2-2 synergies in 4D to the 2 synergies in 8D muscle space to answer the first question and we could not assemble the 8D muscle activity synergies from the left 4D and right 4D synergies. Assembling in this context means that the 4 coordinates of a left sided synergy vector and the 4 coordinates of a right sided synergy vector is concatenated to get an 8-dimensional vector.

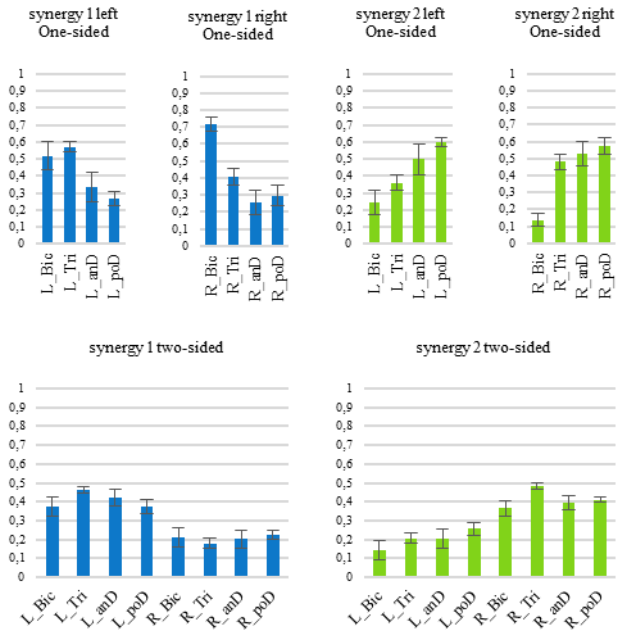

2. Figure Comparison of one-sided synergies with two-sided synergies for unconnected cranking condition. The two-sided synergies cannot be assembled (concatenated) from the one-sided synergies.

We found axial symmetry when 8D synergy vectors were compared (Figure 3.)

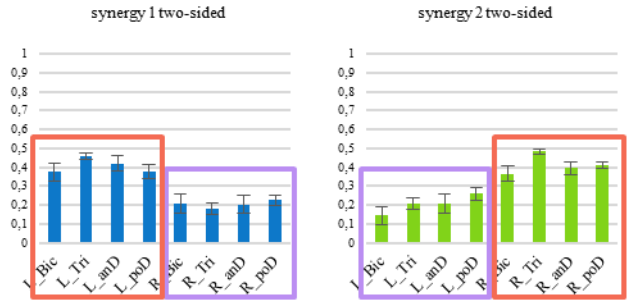

3. Figure Two-sided synergies. These synergies show axial symmetries, the weights of synergy1 in the red box are similar the weights of synergy 2 in red box. The weights in purple box are similar, too.

We note that there were symmetric pairs of synergies when we studied four synergies instead of two in the case of cranking with physically connected cranks.

IV. Conclusion

Our results may reflect the symmetry of bimanual arm cranking movement. This method can give insight into some features of bimanual control. The finding that the bimanual (two-sided) synergies can not be assembled from one-sided synergies supports that the two arms are controlled not independently. When the handles of an arm-cycle ergometer are physically connected than the control of one arm (e.g. the dominant arm) may be the important and the other arm may just "travel" with the dominant arm. Although, our results were found in this case and in that case also, when the two handles (and indirectly the cranks) were not physically connected. In either case we assume that one–sided synergies do not give adequate information about neural control, but two-sided synergies may discern synergistic control in bimanual cranking.

References

[1] L. Botzheim, M. Mravcsik, I. Zsenak, D. Piovesan, J. Laczko (2019) *Jerk decomposition during bimanual independent arm cranking*. In the Proceedings of the International Conference on Rehabilitation Robotics (ICORR) 2019, Torino, Canada.

[2] Sz. Malik, M. Mravcsik, L. Botzheim, A. Klauber, N. Zentai, J. Laczko (2017). *Number and strength of muscle synergies in bimanual arm cycling as a function of crank resistance*. Progress in Motor Control XI. Conference,2017.07.20-22. Miami USA.

[3] Filipe O. Barroso, Diego Torricelli, Elisabeth Bravo-Esteban, Julian Taylor, Julio Gómez-Soriano, Cristina Santos, Juan C. Moreno, José L. Pons, "*Muscle Synergies in Cycling after Incomplete Spinal Cord Injury: Correlation with Clinical Measures of Motor Function and Spasticity"*Front Hum Neurosci. 2015; 9: 706. Published online 2016 Jan 11. doi: 10.3389/fnhum.2015.00706

[4] Filipe O. Barroso, Diego Torricelli, Juan C. Moreno, Julian Taylor, Julio Gomez-Soriano, Elisabeth Bravo-Esteban, Stefano Piazza, Cristina Santos, José L. Pons, „*Shared muscle synergies in human walking and cycling*" J Neurophysiol. 2014 Oct 15; 112(8): 1984–1998. Published online 2014 Jul 23. doi: 10.1152/jn.00220.2014.

Mutual comparison of different classifiers in segmentation of motor unit spike trains identified from high-density surface electromyograms

Aljaž Frančič, Aleš Holobar, and Milan Zorman

***Abstract*—We systematically tested seven different classification algorithms for segmentation of motor unit (MU) firings in the spike trains assessed by Linear Minimum Mean Square Error (LMMSE) estimator from synthetic high-density surface electromyograms (HDEMG). Two different cross-validation schemes were tested: 1) across time with classifiers optimized to each individual MU spike train and 2) across MUs with classifiers optimized for individual muscle contraction. In the first scheme all algorithms produced the same precisions, while Bagging (KNeighbors) produced the best sensitivity across different PNRs. In the second scheme, AdaBoost, KNeighbors, Bagging (KNeighbors), Bagging (RandomForest) and Voting achieved the best precisions, while RandomForest achieved the best sensitivity across different PNRs. Some of the results were significantly different according to the Friedman test ($p < 0.05$). Specificity was the same in all the tested cases.**

I. Introduction

NUMEROUS blind source separation (BSS) algorithms have been proposed to identify motor unit (MU) firing pattern from high-density surface electromyograms (HDEMG) [3]. They all build on the two-step procedure. In the first step, they blindly estimate MU filter, which, when applied to HDEMG signals, yields MU spike trains. In the second step, this spike train is segmented in order to separate the base line noise in the identified spike train from true MU firings (spikes). Namely, as shown in [4] when identified by BSS algorithm, spike train contains the base-line noise consisting of MUs' contributions with similar motor unit action potential (MUAP) shapes and of instrumental noise. Many research studies focused on the optimization of the MU filter, that is on the first step of the MU firing identification [3], whereas the second step received much less attention. In this study, we mutually compared different segmentation techniques for identification of MU firings from the spike trains identified by Linear Minimum Mean Square Error (LMMSE) estimator.

II. Methods

A. Description of synthetic HDEMG signals

Synthetic HDEMG signals were generated using the cylindrical volume conductor model proposed in [1]. 100 MUs with size following Henneman principle were randomly distributed in a muscle tissue, with average fiber density of 20 fibres/mm^2. Fiber length was set to 130 ± 5 mm. MUAP conduction velocities were normally distributed with mean of 4.0 ± 0.3 m/s. MU firing pattern were generated by model proposed in [2], with parameters adjusted for biceps brachii muscle. Constant 10 % excitation level was simulated.

Array of 10×9 electrodes with 1 mm radius and 5 mm inter-electrode distance was simulated. Additive Gaussian noise was added to the 10 s long HDEMG signals, with the Signal-to-Noise Ratio (SNR) set to ∞, 20 and 10 dB. For SNR 20 dB and 10 dB, 5 different noise realizations were tested.

B. Description of LMMSE estimator

LMMSE estimator of the MU spike train is defined by [3]:

$$\hat{t}_j(n) = \mathbf{c}_{t_j,\boldsymbol{y}}\mathbf{C}_{\boldsymbol{y}}^{-1}\boldsymbol{y}(n) \quad (5)$$

where $\boldsymbol{y}$ is a matrix of HDEMG measurements, extended by factor 10 [3], $\boldsymbol{y}(n)$ is its n-th column. $\mathbf{C}_{\boldsymbol{y}} = E(\boldsymbol{y}(n)\boldsymbol{y}^T(n))$ and $\mathbf{c}_{t_j,\boldsymbol{y}} = E\left(t_j(n)\mathbf{y}^T(n)\right)$ where E stands for mathematical expectation.

In our tests LMMSE estimator identified 37 MUs, 8.00 ± 0.63 MUs and 4.40 ± 0.49 MUs at SNR of ∞, 20 and 10 dB, respectively.

C. Description of classifiers

Amplitudes of spikes in $\hat{t}_j(n)$ were used as a classification feature. Supervised learning was chosen to accomplish the given task as it offers a wide palette of methods suitable for our purpose. The following classifiers implemented in scikit-learn for Python [5] (version 0.20.2) were tested:

AdaBoost with the number of estimators set to 100. This meta-algorithm combines the outputs of weak learners – in our case decision trees with the depth of 1 – into a weighted sum, which is the final output of the boosted classifier. ***KNeighbors*** using the default parameters. This is an implementation of the classic k-nearest neighbors algorithm. ***DecisonTree*** using the default parameters. ***RandomForest*** with the number of estimators set to 100. This is an implementation of the random decision forest ensamble learning method, which constructs a multitude of decision trees at training time and outputs the mean prediction of individual trees. ***Bagging (KNeighbors)*** with the default parameters. This is an implementation of the bootstrap aggregating machine learning ensemble meta-algorithm using the aforementioned KNeighbors classifier as the base estimator. ***Bagging (RandomForest)*** with the number of estimators in the random forest set to 100. ***Voting*** classifier was used with the three estimators being AdaBoost, RandomForest and KNeighbors with the same parameters as described above.

This study was supported by the Slovenian Research Agency (projects J2-1731 and L7-9421 and Programme funding P2-0041).

Aljaž Frančič, Aleš Holobar and Milan Zorman are with the Faculty of Electrical Engineering and Computer Science, University of Maribor, Maribor, Slovenia (corresponding author: aljaz.francic@um.si)

D. Description of cross-validation used

Cross-validation ***across time*** was applied by using K-fold method from scikit-learn library [5], where K was set to 5. Each of the identified MUs were treated separately and one fifth of the spike train $\hat{t}_j(n)$ was used for testing, while the rest was used for classificator training. This was repeated with a different part of the spike train used for testing each time.

Cross-validation ***across MUs*** used the K-fold method with K set to the number of identified MUs. All K spike trains were concatenated into a single train, which was sent to the K-fold method. This resulted in one MU spike train always being used for testing whereas the others were used for training.

All spike trains were post-processed to remove consecutive spike occurrences. A tolerance of 1 ms was used when determining true-positive (TP), false-positive (FP) and false-negative (FN) spikes. In the sequel, we report the mean ± SD for precision, sensitivity and specificity of classifiers. The hypothesis of normal distribution of the results was rejected by the Lilliefors test. Therefore Friedman test was used for statistical comparison. All significant effects were corrected by Bonferroni test with significance level set to $p < 0.05$.

III. Results

Specificity was 100 ± 0 % in all the test cases. Precision and sensitivities are reported separately for each tested cross-validation method.

A. Cross-validation across time

TABLE I: PRECISION (CROSS-VALIDATION ACROSS TIME)

Algorithm	Precision		
	SNR = 10	SNR = 20	SNR = ∞
AdaBoost	1.00 ± 0.00	1.00 ± 0.00	1.00 ± 0.00
KNeighbors	1.00 ± 0.00	1.00 ± 0.00	1.00 ± 0.00
DecisonTree	1.00 ± 0.00	1.00 ± 0.00	1.00 ± 0.00
RandomForest	1.00 ± 0.00	1.00 ± 0.00	1.00 ± 0.00
Bagging (KNeighbors)	1.00 ± 0.00	1.00 ± 0.00	1.00 ± 0.00
Bagging (RandomForest)	1.00 ± 0.00	1.00 ± 0.00	1.00 ± 0.00
Voting	1.00 ± 0.00	1.00 ± 0.00	1.00 ± 0.00

TABLE II: SENSITIVITY (CROSS-VALIDATION ACROSS TIME)

Algorithm	Sensitivity		
	SNR = 10	SNR = 20	SNR = ∞
AdaBoost	0.79 ± 0.10	0.84 ± 0.11	0.97 ± 0.05
KNeighbors	0.80 ± 0.12	0.86 ± 0.10	0.98 ± 0.04
DecisonTree	0.80 ± 0.08	0.84 ± 0.10	0.97 ± 0.05
RandomForest	0.81 ± 0.08	0.84 ± 0.10	0.97 ± 0.05
Bagging (KNeighbors)	0.81 ± 0.11	0.86 ± 0.10	0.98 ± 0.04
Bagging (RandomForest)	0.81 ± 0.11	0.85 ± 0.10	0.98 ± 0.04
Voting	0.79 ± 0.09	0.84 ± 0.11	0.97 ± 0.05

B. Cross-validation across motor units

TABLE III:
PRECISION (CROSS-VALIDATION ACROSS MOTOR UNITS)

Algorithm	Precision		
	SNR = 10	SNR = 20	SNR = ∞
AdaBoost	1.00 ± 0.00	1.00 ± 0.00	0.99 ± 0.05
KNeighbors	1.00 ± 0.00	1.00 ± 0.00	0.99 ± 0.05
DecisonTree	1.00 ± 0.01	0.99 ± 0.02	0.99 ± 0.05
RandomForest	1.00 ± 0.01	0.99 ± 0.02	0.99 ± 0.05
Bagging (KNeighbors)	1.00 ± 0.00	1.00 ± 0.00	0.99 ± 0.05
Bagging (RandomForest)	1.00 ± 0.00	1.00 ± 0.01	0.99 ± 0.05
Voting	1.00 ± 0.00	1.00 ± 0.00	0.99 ± 0.05

TABLE IV:
SENSITIVITY (CROSS-VALIDATION ACROSS MOTOR UNITS)

Algorithm	Sensitivity		
	SNR = 10	SNR = 20	SNR = ∞
AdaBoost	0.42 ± 0.41	0.27 ± 0.41	0.66 ± 0.41
KNeighbors	0.51 ± 0.31	0.54 ± 0.32	0.63 ± 0.36
DecisonTree	0.62 ± 0.24	0.65 ± 0.25[A]	0.67 ± 0.31
RandomForest	0.63 ± 0.25	0.67 ± 0.25[A]	0.68 ± 0.30
Bagging (KNeighbors)	0.50 ± 0.32	0.52 ± 0.33[B]	0.63 ± 0.36
Bagging (RandomForest)	0.54 ± 0.29	0.59 ± 0.30[A]	0.65 ± 0.34
Voting	0.47 ± 0.34	0.46 ± 0.34[B]	0.64 ± 0.37

Significantly different from [A]AdaBoost, [B]RandomForest
(Friedman test, $p < 0.05$)

IV. Discussion

All the tested algorithms proved to be highly specific as the number of FPs was relatively small, regardless the tested cross-validation methodology (Tables I and III). On the other hand, the sensitivity of tested classifiers depended significantly on the SNR. In the noiseless cross-validation across time more than 97 % of MU spikes were detected by all the tested classifiers. These figures decrease to about 85 % and 80 % with SNR of 20 dB and 10 dB, respectively.

In cross-validation across MUs, we observed a significant drop of performance in all the classifiers. On average, only around 65 % of MU spikes were segmented in noiseless case. These figures further decreased for 20 dB noise where Adaboost yielded significantly worse sensitivity than DecisionTree, RandomForest and Bagging (RandomForest) while RandomForest was significantly better than Bagging (KNeighbors) and Voting. Interestingly, at 10 dB noise the sensitivities of tested classifiers were not significantly different anymore.

V. Conclusion

We systematically tested the suitability of different supervised learning algorithms for segmentation of MU spikes from raw results of LMMSE estimator of MU spike trains from HDEMG signals. When learned on a specific MU spike train (cross-validation across time), all the algorithms seem suitable for the given task. However, the segmentation learning cannot easily be generalized across different MUs, mainly due to its low sensitivity. Therefore, supervised learning scheme needs to be applied separately to each individual MU spike train. The selection of specific classifier seems to be less important.

References

[1] D. Farina, L. Mesin, S. Martina, R. Merletti, "A surface EMG generation model with multilayer cylindrical description of the volume conductor", IEEE Trans Biomed Eng vol. 51, pp. 415–426, 2004.

[2] A.J. Fuglevand, D.A.Winter, A.E.Patla, "Models of recruitment and rate coding organization in motor-unit pools," J. Neurophysiol. 70, pp. 2470–88, 1993.

[3] A. Holobar and D. Zazula, "Multichannel Blind Source Separation Using Convolution Kernel Compensation", *IEEE Trans Signal Processing*, vol. 55, no. 9, pp. 4487-4496, 2007.

[4] A. Holobar, M. Minetto and D. Farina, "Accurate identification of motor unit discharge patterns from high-density surface EMG and validation with a novel signal-based performance metric", Journal of Neural Engineering, vol. 11, no. 1, p. 016008, 2014.

[5] *"scikit-learn"*. Accessed on: Aug. 7. [Online]. https://scikit-learn.org

PAIRED ASSOCIATIVE STIMULATION FOR MEMORY FACILITATION

A. San Agustín and Jose L. Pons

***Abstract*—Paired Associative Stimulation (PAS) along with rTMS protocols induces cortical plasticity, changes in synaptic strength and function potentiation. However, these changes have been mostly investigated in relation to the nervous motor system. In this review, we detail a brief variety of PAS intervention protocols that facilitate the cognitive process of Memory, which have referred to an explicit PAS application.**

I. Introduction

TRANSCRANIAL magnetic stimulation generates short high intensity magnetic fields, which trespass the cranium and elicit electric currents in the cerebral cortex. The triggered currents induce an activation in nervous cells from small regions. This magnetic stimulation is useful for the assessment of corticospinal motor pathway excitability due to its capability of producing muscle fibres activation that in resting muscle reflects the excitability and local density of the pathway neurons [1].

Moreover, TMS can be utilized in order to induce neuroplasticity-derived changes in nervous system. There are diverse strategies of TMS application to induce neuronal plasticity that can be classified in two broad subgroups: 1. Repetitive TMS (rTMS): a train of TMS pulses typically between 1Hz and 50Hz applied at the same intensity and cortical area [2]. 2. Paired Associative Stimulation (PAS): the combination of a single TMS pulse with another stimulus or event that induce an activation in the same nervous tract. The Hebb's principles explain the effectiveness of PAS application, due to the description of the mechanisms involved in synaptic efficacy changes [3, 4]. Besides, PAS protocols are defined as spike-timing-dependent plasticity (STDP) paradigms for the importance of time precision in stimuli convergence [5].

Within the PAS paradigm, there are also different protocols, which differ in the stimulus or event that triggers cortical activity coupled with the TMS pulse [6]. To our knowledge, the first time that a PAS protocol is applied, the pulse of TMS in motor cortex is paired with an electrical stimulus in the medial nerve with an Inter Stimulus Interval (ISI) of 25ms [4], determining a peripheral-cortical PAS (pc-PAS) protocol.

Subsequently, other protocols converging stimuli have emerged. Pairing two TMS pulses, one in each hemisphere, conducted cortico-cortical PAS (cc-PAS) protocol, also called Paired Bihemispheric Stimulation (PBS) [7, 8], and pairing TMS pulse with genuine activation of cortex driven by the performance of a movement related motor task, characterizing the task-related PAS protocol [9, 10].

This latter stimulation protocol for the plasticity induction opens the door to the PAS application in cortical areas beyond the sensory-motor cortex, where the vast majority of PAS studies have been focused so far.

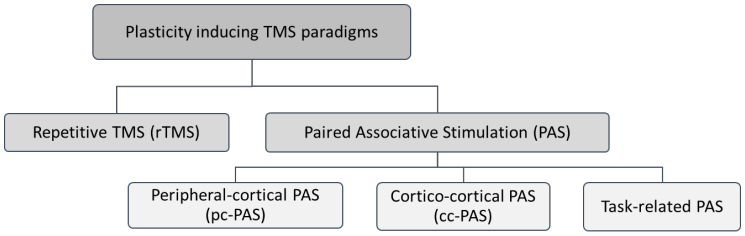

Fig. 1. Scheme of plasticity inducing TMS protocols taxonomy mentioned in this review.

With the possibility of matching TMS with neuronal activity triggered by a task, the cortical areas related to cognitive processes, which do not have a direct afferent pathway that can be electrically activated, are susceptible to their potentiation with the requirement of being attainable by the TMS magnetic field. Thus, the pulse of TMS and the endogenous activation of the cortical area could converge for its facilitation.

In any case, there have been studies following other strategies in the application of PAS that have obtained results related to cognitive processes such as learning and memory. In this review we wanted to focus on this cognitive process and show how applying different PAS protocols it is possible to induce plastic changes also in relation to Memory.

II. Materials and Methods

We performed a systematic search on PubMed database in September 2019, with the words "Paired Associative Stimulation" and "Memory" in the Title or Abstract. We obtained 37 publications of which eight defined a PAS intervention with results directly related to the facilitation of memory. We discarded articles that, although they adhered to these requirements, were not applying the intervention explicitly to facilitate memory process but to compare the ability to induce plasticity between different groups (i.e., patients and healthy subjects). Finally, only three papers adhered to our requirements; the ones described in this review.

A. San Agustín is with the Neurorehabilitation Group at Cajal Institute of the Spanish National Research Council, Madrid, Spain (asanagustin@caja.csic.es) and Jose L. Pons is with the Shirley Ryan AbilityLab, Chicago (IL), USA.

TABLE I
STUDIES REPORTING MEMORY FACILITATION RELATED TO A PAS INTERVENTION

PAS Intervention	Reference	Stimuli localization	PAS Effects
Pc-PAS	Yan Hu (2019)	TMS: Right Motor Cortex PNS: Left Tibial Nerve	Learning and memory performance improved; in hippocampus: cerebral ultrastructure restored, synaptic plasticity enhanced, BDNF and NMDA upregulated.
	Rajii et al. (2013)	TMS: Lateral Prefrontal Cortex (LPFC) PNS: Right Median Nerve	Potentiation of CEA, enhancement of γ- and θ-activity and θ-phase-γ-amplitude coupling (related to working memory).
Cc-PAS	Camila L. Nord et al. (2019)	TMS : Lateral Prefrontal Cortex (LPFC) TMS : Intraparietal Sulcus (IPS)	Shifted sequential learning task control.

III. PAS PROTOCOLS INDUCING MEMORY-RELATED PLASTIC CHANGES

A. Pc-PAS protects cognition after cerebral ischemia.

The pc-PAS protocol is based on the synchronization of a single TMS pulse related with a low-frequency peripheral nerve stimulation. Yan Hun et al. (2019) applied 0.05 Hz electric pulses in the left tibial nerve of a rat model of cerebral ischemia, paired with TMS pulse in right motor cortex, 90 times each day during 4 weeks. Although the intervention is applied at motor pathway, they found facilitation related with hippocampal cells and learning and memory performance. Pc-PAS significantly improved learning and memory in Morris water maze performance, synapses that had a damaged structure in region CA1 of hippocampus were restored, LTP induced synaptic plasticity was enhanced in CA1 and CA3 regions and finally, BDNF and NMDAR1proteins were upregulated [11]. This pc-PAS protocol study showed that tibial motor cortex PAS facilitation influenced hippocampal area, generating an additional facilitation in learning and memory.

B. Cc-PAS shifted the control type in a sequential learning task.

The cc-PAS protocol consists of pairing two transcranial magnetic single pulses from different TMSs applied each in different cortical locations. Camila L. Nord et al. (2019) followed a ccPAS protocol pairing a TMS pulse in right Intraparietal Sulcus (IPS) with another TMS pulse in right Lateral prefrontal cortex (LPFC), with an ISI of 10ms. 100 pulses were applied in both directions, IPS being firstly stimulated (IPS→LPFC) and in the opposite direction (LPFC→PPS). After the stimulation, the subjects performed a sequencing learning task, in which subjects had to choose symbols in two stages for a monetary reward outcome. Regarding the IPS→LPFC, there were changes in the control performed during the sequential learning task. The subjects after the cc-PAS shifted from a habitual control, focusing on the reward of previous trial (model free based), to following a factor of transmission between task levels (model based), which is a goal directed control [12]. This cc-PAS protocol study showed that its application could change the behavior dealing with a sequential learning task.

C. Ps-PAS in DLPF potentiates cortical excitability.

Following a pc-PAS protocol does not mean that peripheral stimulation has to be paired with TMS motor cortex stimulus. Tarek K Rajji et al. (2013) paired peripheral nerve stimulation of the right median nerve with TMS to the human left dorsolateral prefrontal cortex (DLPF), with an ISI of 25ms. As potentiation marker analogous to Motor Evoked Potential (MEP), they record the cortical evoked activity (CEA), defined as the area under the curve of the rectified single pulse TMS-evoked potential (TEP). The intervention based on this protocol resulted in spatial and frequency specific enhancement of CEA in DLPF, meaning a potentiation in cortical excitability, a potentiation within γ- and θ-frequency bands and their coupling. The coupling of these frequency bands are associated to working memory related activity, which likely represented a neuronal network and synapsis activation during DLPF engagement to a working memory task [13]. The intervention of this study suggest that ps-PAS in a different location than motor cortex, can result in cortical excitability potentiation too and in DLPF can be applied as working memory enhancement strategy.

IV. CONCLUSION AND DISCUSSION

These findings suggest that PAS-TMS interventions have a potential use for improving cognitive processes, in concrete, learning and memory.

To our knowledge, there are more studies that applied a PAS-type intervention [14, 15, 16] but the PAS term had not been utilized or the procedimental methods are equals to PAS, although they are not recognized as such. Since Stefan et al. in 2000 [4] coined the term, only these three studies have had results concerning memory changes when applying PAS, making explicit reference to the term. Thus, a review of implicit PAS intervention studies will be necessary to compile all the studies that have combined TMS with another activating stimulus in a synchronized way and with repercussion in the memorization process (whether at the cellular level or at the behavioral level). In this way, a broader data regarding the PAS interventions that have been conducted so far and their consequences in relation to memorization will be achieved.

REFERENCES

[1] Hallett, M. (2000). Transcranial magnetic stimulation and the human brain. Nature, 406(6792), 147.

[2] Rotenberg, A., Horvath, J. C., & Pascual-Leone, A. (Eds.). (2014). Transcranial magnetic stimulation. New York: Springer.

[3] Hebb, D. O. (1949). The organization of behavior; a neuropsycholocigal theory. A Wiley Book in Clinical Psychology., 62-78.

[4] Stefan, K., Kunesch, E., Cohen, L. G., Benecke, R., & Classen, J. (2000). Induction of plasticity in the human motor cortex by paired associative stimulation. Brain, 123(3), 572-584.

[5] Markram, H., Lübke, J., Frotscher, M., & Sakmann, B. (1997). Regulation of synaptic efficacy by coincidence of postsynaptic APs and EPSPs. Science, 275(5297), 213-215.

[6] San Agustín, A., & Pons, J. L. Paired associative stimulation protocols with transcranial magnetic stimulation for motor cortex potentiation. In SCHOOL AND SYMPOSIUM ON ADVANCED NEUROREHABILITATION (SSNR2018) (p. 44).

[7] Rizzo, V., Siebner, H. S., Morgante, F., Mastroeni, C., Girlanda, P., & Quartarone, A. (2008). Paired associative stimulation of left and right human motor cortex shapes interhemispheric motor inhibition based on a Hebbian mechanism. Cerebral cortex, 19(4), 907-915.

[8] Koganemaru, S., Mima, T., Nakatsuka, M., Ueki, Y., Fukuyama, H., & Domen, K. (2009). Human motor associative plasticity induced by paired bihemispheric stimulation. The Journal of physiology, 587(19), 4629-4644.

[9] Thabit, M. N., Ueki, Y., Koganemaru, S., Fawi, G., Fukuyama, H., & Mima, T. (2010). Movement-related cortical stimulation can induce human motor plasticity. Journal of Neuroscience, 30(34), 11529-11536.

[10] San Agustín, A., Asín-Prieto, G., & Pons, J. L. (2018, October). Fatigue Compensating Muscle Excitability Enhancement by Transcranial Magnetic Stimulation: A Case Report. In International Conference on NeuroRehabilitation (pp. 839-843). Springer, Cham.

[11] Hu, Y., Guo, T. C., Zhang, X. Y., Tian, J., & Lu, Y. S. (2019). Paired associative stimulation improves synaptic plasticity and functional outcomes after cerebral ischemia. Neural regeneration research, 14(11), 1968.

[12] Nord, C. L., Popa, T., Smith, E., Hannah, R., Donamayor, N., Weidacker, K., ... & Voon, V. (2019). The effect of frontoparietal paired associative stimulation on decision-making and working memory. Cortex, 117, 266-276.

[13] Rajji, T. K., Sun, Y., Zomorrodi-Moghaddam, R., Farzan, F., Blumberger, D. M., Mulsant, B. H., ... & Daskalakis, Z. J. (2013). PAS-induced potentiation of cortical-evoked activity in the dorsolateral prefrontal cortex. Neuropsychopharmacology, 38(12), 2545.

[14] Cattaneo, Z., Vecchi, T., Pascual-Leone, A., & Silvanto, J. (2009). Contrasting early visual cortical activation states causally involved in visual imagery and short-term memory. European Journal of Neuroscience, 30(7), 1393-1400.

[15] Hannula, H., Neuvonen, T., Savolainen, P., Hiltunen, J., Ma, Y. Y., Antila, H., ... & Pertovaara, A. (2010). Increasing top-down suppression from prefrontal cortex facilitates tactile working memory. Neuroimage, 49(1), 1091-1098.

[16] Rose, N. S., LaRocque, J. J., Riggall, A. C., Gosseries, O., Starrett, M. J., Meyering, E. E., & Postle, B. R. (2016). Reactivation of latent working memories with transcranial magnetic stimulation. Science, 354(6316), 1136-1139.